DUPLICATE

METEOROLOGICAL OFFICE
14 APR 1994
LIBRARY

Forecasting Research

Forecasting Research Division
Technical Report No. 89

The assimilation of ERS-1 scatterometer winds

by

R.S. Bell

March 1994

Meteorological Office
London Road
Bracknell
Berkshire
RG12 2SZ
United Kingdom

ORGS UKMO F
National Meteorological Library
FitzRoy Road, Exeter, Devon. EX1 3PB

Forecasting Research Division
Technical Report No. 89

The assimilation of ERS-1 scatterometer winds.

by R.S. Bell

March 1994

Forecasting Research Division
Meteorological Office
London Road
Bracknell
Berkshire, England

Note: This paper has not been published. Permission to quote from it must be obtained from an Assistant Director of the above Met Office Division. An abbreviated version was presented to the 2nd ERS-1 Symposium in Hamburg during October 1993 (see references below for details)

© Crown Copyright 1994

1. Introduction

ERS-1 was launched in mid 1991 with a package of instruments designed to observe various aspects of the earth's surface. The instrument of most interest to meteorology is the AMI scatterometer which provides wind measurements over the oceans by measuring the radar back-scatter from ocean capillary waves at three look directions. In section 2, we briefly described aspects of the data processing, as well as some recent data monitoring results. The data monitoring activity has been continuous since launch. Results from this monitoring, combined with some preliminary impact studies (Bell and Holt, 1993) have led to improvements in all stages of the processing and assimilation. Following final algorithm calibrations in January 1993, a pre-operational trial was run during March 1993. In this trial, scatterometer winds were included in the global assimilation in addition to observations from other sources already used operationally. The method of assimilating the scatterometer data is discussed in section 3 and the results of the impact study follow in section 4. As a result of this trial, the scatterometer data having produced a positive impact, were included within the global operational data assimilation on 4th August 1993.

2.1 Data preprocessing

The triplet of calibrated back-scatter (σ_0) measurements can be related to a wind speed and direction using an empirical transfer function (Stoffelen and Anderson, 1993). Because of the cyclical nature of the transfer function with wind direction, the result of such a retrieval is 4 ambiguous wind directions of which the upwind and downwind directions usually have a high (but near equal) likelihood. The correct direction can only be satisfactorily resolved using additional information, eg from a forecast model. For this reason we have chosen to do the wind retrieval in-house so that we can make use of the most up to date model background winds as an integral part of this ambiguity removal. In the algorithm development phase this strategy had the additional benefit of allowing the introduction of new retrieval algorithms in a more timely manner than was achieved by ESA.

Details of the processing are given in Offiler (1990). In brief, the three stage procedure starts with the ambiguous winds being ranked according to their 'goodness of fit' or residual to the σ_0 function - this is the weighted sum of squares of the difference between the measured σ_0 values and those given by the function for that particular wind vector. The model background is brought in at the second stage where the rank 1 solution is retained if it is nearest background, otherwise other solutions are considered. The final stage consists of a nearest neighbour test to check for local consistency.

The σ_0 to wind processing implicitly includes some quality control, by virtue of its use of a model background and local consistency checks. Prior to assimilation, a further check using a Bayesian methodology is included which uses a more timely background field. Additional constraints on the observed divergence have been tested to filter out some of the remaining incorrect ambiguities. In our tests, less than 1% of the data are flagged in the final quality control check.

Based on results from our data monitoring work, we also permanently reject some of the cells within the swath. We are careful not to include any data from areas thought be ice

covered (based on JIC Washington ice analyses). We eliminate all reports based on less than 3 look directions. We also choose to reject all reports from the inner edge of the swath which seem less reliable.

2.2 Coverage

The final product of the data preprocessing is a 500 km wide swath of wind vectors, with 19 overlapping 50 km cells across the swath at a separation of 25 km. With this swath width, one third of the earth's ocean area is observed in a day. In reality the coverage is somewhat less than this because an important part of the ERS-1 mission is dedicated to another instrument, the SAR, which cannot operate in tandem with the scatterometer. This reduced the data coverage in the northern latitudes (north of 30°N) and particularly the North Atlantic, as we saw during our trial (the details of which are given below in section 4.1). Average data volumes during our trial were some 17000 reports per day in the northern hemisphere extra-tropics (90°N-30°N), 74000 reports per day in the tropical band (30°N-30°S) and 67000 reports per day south of 30°S. It is worth noting that in these three areas, the ice free sea area as a percent of the global area is 6%, 37% and 20% respectively during March. If northern hemisphere coverage were as good as that in the southern hemisphere, we would expect 6/20 of 67000 reports north of 30°N, where as in fact significantly fewer were available. This is a worst case position for northern hemisphere data availability since the ice extent is at a maximum there during March.

Figure 1 shows a 24 hour coverage map for 21st March 1993, to illustrates the coverage that was being achieved during the trial. The 'one third per day' coverage is highlighted, as is the occasional missing orbit. We also see gaps in the orbits where the instrument has been temporarily disabled, for example the three orbits in the North Atlantic between 0° and 40° west. Figure 2 shows the cumulative data density during the full 10 days of the trial as a percentage of the maximum data density. Note the density nearest the poles is typically twice that in the equatorial latitudes because the swaths converge near the poles. Also note that the gaps in the orbits to the west of the UK were a persistent feature during the period.

2.3 Quality

Maps of the UKMO scatterometer winds have been made available to the Central Forecast Office since soon after launch, and have been well received; the quality being good and the occasion of incorrect wind directions being few. Although lack of data over meteorologically important features has caused frustrations. Small-scale low pressure systems (both extra-tropical and tropical) and trough lines have been identified with considerable extra detail compared with model background plots. The forecasters have also been happy with the wind strengths in the high wind regimes. The subjective assessment has been backed up by a comprehensive monitoring exercise which has been ongoing since launch. Observation differences from model background, broken down by speed, latitude and swath position, have yielded important feedback to the algorithm calibration, as well as demonstrating the quality of the product relative to ship data.

A comprehensive study of ship, buoy and scatterometer wind data has been part of the regular monitoring activities within the Central Forecasting division. During the period since

ERS-1 launch we have noted the steady improvement in scatterometer quality. Since the final engineering calibrations in Spring 1992, our retrieved scatterometer winds have consistently bettered ship winds in all respects (Smith and Waters, 1992). Results for the most recent comparison for Spring 1993, including the period of the pre-operational trial are given in Tables 1 and 2, where scatterometer data is compared indirectly with ship data. Only a subset of all the available ship data has been chosen for this statistical comparison. We imposed a strict quality control whereby only those ships reporting at least 7 times per month which have an rms vector wind difference from background of less than 6 m/s are used. This sample of 'good' ships includes half of all ship reports. The cutoff of 6 m/s was chosen to be 50% greater than the annual difference from background of Ocean Weather Ship GACA (and approximately equal to the largest monthly difference for this ship in the stormiest months). The background values are at 10 m for the scatterometer and 25 m for the ships, which correspond approximately with the observation heights.

		No. of Obs -1000's	Mean obs speed (m/s)	Mean speed diff. (m/s)	s.d. speed diff. (m/s)	Mean dir. diff. (deg)	s.d. dir. diff. (deg)	r.m.s. vector diff. (m/s)
NH	scat.	495	8.5	0.0	2.1	-1.7	21.9	3.4
	ship	24	9.0	0.5	3.1	-3.1	30.2	4.6
TR	scat.	1937	5.5	0.0	1.6	-0.7	23.5	2.6
	ship	20	6.7	0.5	2.5	-0.9	32.5	3.9
SH	scat.	1714	8.1	-0.2	2.6	1.9	27.6	4.2
	ship	2.6	7.7	0.3	3.1	3.4	34.8	4.8
GL	scat.	4145	6.9	-0.1	2.1	0.3	25.2	3.5
	ship	47	7.9	0.5	2.9	-1.9	31.4	4.3

Table 1 : Ship and scatterometer differences from model background as a function of latitude for March 1993

In table 1, we breakdown the statistics into different latitude bands (60° intervals for northern hemisphere [NH], tropics [TR} and southern hemisphere [SH]) as well as giving the global figures [GL]. The standard deviations of wind speed and wind direction differences from model background and the rms vector wind difference all show the scatterometer data to be of substantially higher quality than ship data in all areas. Outside the southern hemisphere the rms difference from background is one third lower for scatterometer observations than for this sample of the better ship reports. In the southern hemisphere the difference is less

marked because the component of background error in the (observation - background) difference is that much greater. The global speed bias is close to zero for the scatterometer data, whereas ship data are 0.5 m/s stronger than background on average. The statistics for the tropical band show a disagreement in the mean observed and background wind speeds which is probably the result of a sampling discrepancy.

In table 2, the same data is broken down by five speed bins, and the same picture emerges. In the lowest speed bin, the direction statistics are not calculated for speeds less than 4 m/s. One interesting feature is that at all but the lowest speed range the scatterometer winds are weaker than the model background whereas the ship winds are stronger, even after accounting for possible differences in reporting height. Even after eliminating many of the more unreliable reports, we suspect that ships have a tendency whether due to poor exposure or a bias towards gust speeds, to over reports wind speed. Nevertheless, it does seem that at the very highest wind speeds the scatterometer might be biassed low. The standard deviations of wind speed and wind direction differences from model background and the rms vector wind difference are lower for the scatterometer data at all wind speeds.

		No. of Obs -1000's	Mean obs. speed (m/s)	Mean speed diff. (m/s)	s.d. speed diff. (m/s)	Mean dir. diff. (deg)	s.d. dir. diff. (deg)	r.m.s. vector diff. (m/s)
0-5	scat.	1274	3.8	0.2	1.6	0.7	36.2	2.7
	ship	12	3.5	0.0	2.3	-0.9	53.7	3.6
5-10	scat.	2143	7.0	-0.3	2.2	0.1	23.4	3.5
	ship	23	7.5	0.4	2.7	-1.8	29.4	4.2
10-15	scat.	652	11.8	-0.2	2.6	0.8	17.8	4.4
	ship	9	12.5	1.0	3.4	-2.6	18.5	5.0
15-20	scat.	72	16.0	-0.7	2.3	0.8	14.4	4.6
	ship	2	17.4	1.3	4.1	-1.6	14.8	5.9
>20	scat.	1.9	19.9	-2.5	1.8	0.4	10.0	4.9
	ship	0.25	23.4	2.7	4.7	-2.5	12.9	6.8

Table 2 : Ship and scatterometer differences from model background as a function of speed for March 1993

Both tables 1 and 2 show the large difference in data volumes between the two observing

systems. The scatterometer providing 15 times more data in the northern hemisphere and 100 times more data in the southern hemisphere.

3.1 Data assimilation

Atmospheric assimilation is performed using the Met. Office operational analysis correction scheme (Lorenc et. al., 1991). This is an iterative analysis, with each variable being analysed in turn together with appropriate balancing constraints. The model field relaxes towards the observations gradually such as to minimise any imbalances. Each iteration is interleaved with a time-step of the full forecast model to keep the analysis close to the preferred model solution. Observations are introduced into this continuous assimilation over a period around their validity time, with a peak weighting at their validity time. The horizontal spreading is determined by a continuous background error correlation function which has a time dependence such that progressively smaller scales are fitted.

The characteristics of the scatterometer wind observations differ significantly from conventional sources of marine surface wind data. There is the obvious geographical distribution difference; the ships provide a rather haphazard distribution with a focus on coastal waters and regular shipping lanes, whereas of course the scatterometer provides a regular high density of information within the swath and no information outside the swath. There is also a difference in the nominal height of the report. The retrieval algorithms have been tuned to give winds at a nominal 10 m, whereas the ships may or may not have been reduced to 10 m depending on the observing practice (typically we find that ships are better fitted at 25 m). We also need to consider the light wind regime where the scatterometer is unable to provide reliable directional information. Revisions to the data assimilation system have been introduced to account for these different characteristics.

The increments at the observation position are calculated using a modeled 10 m wind. The interpolation to 10 m in the model boundary layer is performed in a manner consistent with the calculation of surface turbulent fluxes, which yields interpolation coefficients which are a function of stability and surface roughness. Below a threshold (4 m/s) the assimilation uses only the speed information. Horizontal correlation scales have been reduced in response to the higher data density. The values chosen are 240 km at the start of the iteration, reducing to 120 km at the observation time. These values are a compromise between our desire to analyses small scale features where they are observed and our desire to spread information into the data voids beyond the swath. The vertical correlation scale has been retuned following a re-examination of (O-B) radiosonde statistics, and for surface data it is defined such that the correlation drops to about 0.7 at 900 hPa and 0.2 at 800 hPa. All observations surviving quality control are used in the assimilation, but at global scales where the model resolution is 90 km, observation data at the density provided by the scatterometer is not required. Our thinning strategy avoids a preliminary sort or averaging by choosing a different subset (one fifth) of the data at each iteration of our analysis (there are 36 iterations in a 6 hour global assimilation). At each iteration, a surface wind increment field is generated making use of all surface observations (scatterometer and surface based reports). Options have been coded to calculate independent increment fields from different observing systems, however these have not found to be necessary. The reduced horizontal correlation scales together with the data thinning strategy, which, whilst retaining all data, reduces the density of scatterometer reports to an extent where they do not swamp ship data. Both of these

measures also contributed to a significant cost saving and help make operational use of the data a reasonable proposition. The cost overhead of assimilating the scatterometer data is estimated to be no more than 10%, although data volumes exceed the sum of all other observing systems combined.

3.2 Derived pressure increments

The operational AC assimilation scheme contains balance steps whereby geostrophically derived wind increments are calculated from the analysed temperature and pressure increments. These balanced increments provide an approximation to a multivariate analysis and help reduce gravity wave noise. The assimilation of a data source of wind only information, such as is provided by the scatterometer, would benefit considerably from the provision of balanced mass field increments based on analysed wind increments. Andrews and Bell (1993) have recently extended the assimilation to derive balanced pressure and temperature increments from the wind increment field. Briefly, this involved the generation of geopotential increments, $\Delta\phi$, from the wind increments, $\Delta\underline{v}$, which is a straight forward process using a global Poisson solver. Streamfunction increments, $\Delta\psi$, are derived from the wind increments:-

$$\Delta\psi = \nabla^{-2}[\hat{\underline{k}} \cdot Curl(\Delta\underline{v})] \qquad (1)$$

A balance equation is then used to derive the geopotential increments. In this case the linear balance equation is used, hence:-

$$\Delta\phi = \nabla^{-2}[\underline{\nabla} \cdot f\underline{\nabla}(\Delta\psi)] \qquad (2)$$

where f is the Coriolis parameter.

Wind increments are available at all 5 model levels below 700 hPa from surface wind data (levels where the vertical structure function is significantly non-zero). This yields geopotential increments at each level, from which we need to generate a surface pressure increment, ΔP_*, and potential temperature increments, $\Delta\theta$ at each level. We require the geopotential increments at half levels which we obtain from a thickness weighted linear interpolation. Then use the hydrostatic equation to calculate the surface pressure increment and the potential temperature increments.

Clearly we have too many unknowns and an additional constraint is required to close the problem. For our closure, we note that in general the temperature of the lowest model level has little to do with the rotational wind component at that level, because of boundary layer processes. We therefore choose to impose the constraint that the temperature increment for the lowest model level be zero (note that the potential temperature increment for this model level will in general be non zero because of the contribution from ΔP_*). A small amount of manipulation of the hydrostatic equation with this constraint yields the following expression for the surface pressure increment.

With this, and the geopotential increments from higher levels, the potential temperature increments above the first level can also be calculated. For our preliminary tests we were more confident of the surface pressure increments than we were of the potential temperature

$$\Delta P_* = \frac{-\Delta \phi_{\frac{3}{2}}}{R\left[\left(\theta_1 \pi_1 - \theta_{\frac{3}{2}} \pi_{\frac{3}{2}}\right)\left(\frac{B}{P}\right)_{\frac{3}{2}} - \frac{\theta_1 \pi_1}{P_*}\right]} \qquad (3)$$

increments. The correlations we obtained from comparison of derived and true increments were an impressive 0.8 in the extra-tropics for surface pressure but were much lower for low level temperatures. For our first implementation we chose to make use of only the derived surface pressure increments. A latitudinally varying correlation function was chosen which reduced as Sin(1.5 *|latitude|) equator-ward of 60°.

4.1 An impact experiment

A global data assimilation was run in parallel with the operational assimilation for an 11 day period from 18th to 28th March 1993. The trial differed from the control in two respects. Scatterometer winds were include and balancing surface pressure increments were included based on the surface wind analysed increments (derived from scatterometer and ship data). The methods adopted being those outlined in section 3 above.

An observation processing database (OPD) was generated, giving diagnostics from the global data assimilation cycle. Forecast verification was available from the 5 day forecast which ran from a 12UTC analysis. A small number of charts were produced to highlight differences between trial and control. Output was provided to drive a parallel wave model.

Unfortunately, two hiccups in data availability occurred. At 06UTC 22nd (due to problems at ESA) and from 06UTC 23rd to 06UTC 24th inclusive (due to Met. Office database problems). As we noted in section 2.2, we obtained three and a half times the observations in the extra-tropical southern hemisphere compared with the extra-tropical northern hemisphere and it follows from this that we might expect a much bigger impact in the southern hemisphere, particularly given the extra value of observations in a usually data sparse region.

4.2 Data assimilation cycle diagnostics

The best measure of the performance of a data assimilation system is the fit of a short period forecast to the next set of observations. We examined these (observation-model background) statistics for all observation types common to both trial and control. The significant differences were all in the extra tropical southern hemisphere and were mostly restricted to the lower levels of the atmosphere. They all presented a positive signal as we see in table 3. We see the typical reduction in rms (o-b) is 3%. To obtain this degree of improvement in the short period forecasts, we must presume that the scatterometer winds are providing a significantly better analysis.

For areas north of 30°S, most statistics (not shown) were the same and where differences did occur they were so small that no significance could be attached to them.

	Trial (o-b)	Control (o-b)
ship pmsl	1.80 hPa	1.85 hPa
synop pmsl	1.46 hPa	1.49 hPa
ship winds	5.13 m/s	5.30 m/s
low level cloud track winds 600-850 hPa	2.60 m/s	2.68 m/s

Table 3: (observation - background) results during trial, pole-ward of 30°S

4.3 Objective forecast verification results

Forecasts were verified at 24 hour intervals by comparison against surface reports and radiosondes of the 12UTC forecast, meaned over standard latitude band verification areas (60° bands labelled NH for 90°-30°N, TR for 30°N-30°S and SH for 30°-90°S). In table 4, we present the results for the southern hemisphere expressed as a percentage change in rms error to simplify the comparison, with trial improvements shown as positive.

	T+24	T+48	T+72	T+96	T+120	Average through f/c
850 hPa height	10.1	9.7	8.4	6.7	3.4	7.7
500 hPa height	6.3	8.5	6.8	4.9	4.0	6.1
250 hPa height	6.2	7.2	6.8	6.3	5.9	5.8
850 hPa temp	2.8	0.6	2.8	2.3	4.7	2.6
500 hPa temp	5.8	2.0	5.0	-1.5	2.8	2.8
250 hPa temp	4.1	1.3	-0.1	-7.4	-6.7	-1.7
850 hPa wind	1.5	1.7	3.1	1.9	3.1	2.2
500 hPa wind	3.9	3.7	1.4	0.7	1.5	2.2
250 hPa wind	1.9	1.5	0.7	0.1	-2.8	0.3
pmsl	7.1	10.1	8.7	8.3	5.2	7.9
Average of all variables	5.0	4.6	4.6	2.2	2.2	3.7

Table 4 : %change in rms score for extra-tropical southern hemisphere forecasts, pole-ward of 30°S. (positive=trial better)

The improvements in the southern hemisphere are substantial. The surface pressure and height fields show improvements in forecast scores of between 6-10% at all forecast ranges out to 4 days. The temperature and wind fields show improvements of between 2-4%. The 250 hPa temperature scores at days 4 and 5 seem anomalous and probably resulted from a quality control difference with the set of verifying observations, because at adjacent levels

above and below 250 hPa the trial was better. Improvements are greatest at the shortest forecast ranges, but much of the improvement is retained out to the medium range. It is interesting to see a rather bigger signal at the surface at 24 hours in table 4, than we saw at 6 hours in table 3. One possible explanation for this is that in data sparse regions 6 hour forecast errors might be correlated with observation errors.

Differences were minimal in the northern hemisphere and tropics. Overall we saw differences less than 0.5%, with the control being marginally better in the northern latitudes and the trial being marginally better in the tropics. No significance can be attached to such small differences.

4.4 A global assessment of the impact

In figures 3-6, we show a typical global difference between the trial and control experiments. Figure 3 gives the analysed vector wind difference at the 10 m level. We see immediately that the largest differences are south of 45°S; up to 20 knots in places. We also see that the differences are not confined to lines of satellite swath, which implies that the data assimilation system is both spreading the information away from the source of the data and is retaining information from past times, as the differences represent the cumulative impact of 10 days assimilation of the scatterometer data. Figure 4 shows the equivalent difference at 850 hPa. The differences between figures 3 and 4 are, for the most part, reasonably well correlated. In some areas differences at 10 m, as in parts of the Pacific in this case, become negligible at the higher level. In other areas, as in the Indian Ocean and parts of the North Atlantic, the 850 hPa differences are as large if not larger than the lower level differences. The equivalent surface pressure difference is given in figure 5. Here we see that significant differences are confined to the area south of 45°S; with a maximum difference of 12 hPa. It is rare that analysis errors exceed 2 hPa in the northern hemisphere, so we would not expect large areas to differ by more than 1 hPa. Figure 6 shows the 3 day forecast surface pressure differences which follow from the analysis difference highlighted in figures 3-5. The northern hemisphere forecast differences did not exceed 4 hPa. This was reasonably typical of most forecasts during the trial, although some days did see larger differences. The southern hemisphere differences have become more widespread, mostly through eastward advection during the forecast.

Figures 7 and 8 show zonal mean height-latitude cross sections of the rms vector wind differences and rms temperature differences of the analyses over the full 10 day period of the experiment. The zonal meaning was taken for sea points only. In the wind cross section, we don't see much vertical gradient to the error differences even though the source of the difference was surface data. In the temperature cross section, the largest differences are near the surface. In both these cross sections the size of the difference is rather small. The global maps of the rms differences show that even averaged over a 10 day period, there are areas where differences are much larger than the zonal average. These might be associated with the most synoptically active areas or perhaps where the data distribution is highest. Figures 9 and 10 illustrate the rms difference in vector wind fields at the surface (10 m) and 850 hPa over the 10 day period. The comparable rms surface pressure difference is given in figure 11. These three figures show error patterns which are not dissimilar to the single case shown in figures 3-5. RMS surface pressure analysis differences in the South Pacific in excess of 4 hPa are perhaps a little surprising and reflect our current degree of uncertainty in that data

void, where a new data source is especially welcome.

4.5 A Subjective assessment in the South Atlantic

Subjective assessment is a problem because in the southern hemisphere, where differences are largest the truth is difficult to determine and as we have seen the differences outside the southern hemisphere storm belt were rather small. The South-West Atlantic is one sector of the southern hemisphere where some reliance can be placed on the objective analysis as there is a reasonable number of surface reports from ships, islands, the southern tip of South America and the Antarctic peninsula further south. It is also an area where forecast differences were largest, being downstream of the South Pacific data void. Figure 12 compares the rms surface pressure difference of trial and control forecasts from verifying operational objective analyses for this sector within 2000 km of southern Argentina. We see the trial 'winning' on 8 occasions out of 10, in some cases by a considerable margin. The two cases where the control operational run had lower scores occurred for forecasts from data times on the 25th and 26th (VT 28th, 29th) following the ERS-1 data problems.

Differences in the synoptic evolution are readily apparent in cases where the objective scores show improvements in the region of 20%. Although even in such cases, the two forecasts are more like each other than they are like the verification. Figures 13-22 each show 6 charts of this south Atlantic area (one for each forecast comparison). The upper charts in each figure show trial and control 3 day forecasts of surface pressure together with the verifying control analysis. The lower charts show differences (trial-verification), (control-verification) and (trial-control). In the remainder of this section, we give a summary of the main differences in synoptic evolution in the area and demonstrate that the trial forecasts prove to validate better in a subjective comparison as well as an objective comparison. The margin in the subjective assessment is roughly 8:2 as for the objective assessment.

Fig 13 - VT 22nd — The trial has more correctly emphasised the low to the south-east of the Falklands rather than second centre south of Cape Horn.

Fig 14 - VT 23rd — Both have mis-handle the developments to the east of Chile. The ridge south of the Falklands is better forecast in the trial which therefore has correctly got the weaker winds at 60°W.

Fig 15 - VT 24th — Both forecasts are out of phase with developments near South America, but the phase of the ridge from the Antarctic peninsula to South Georgia is better in the trial.

Fig 16 - VT 25th — The trial correctly positions the low south of the Falklands, with better direction to the flow south of Tierra del Fuego. The trial also has a better low over the Antarctic peninsula.

Fig 17 - VT 26th — The trial has a better low west of Chile (although both forecasts are too shallow) and is not as slow with the ridge running through the Falklands to Tierra del Fuego. The small low to the east of the Antarctic peninsula is also better in the trial.

Fig 18 - VT 27th — Both forecasts seem to have got the phase of developments wrong but the trial, with low 997 hPa on the South American coast, is a better representation of the 988 hPa low south of the Falklands than the control which has a flabby area with minimum of 1007 hPa over Chile.

Fig 19 - VT 28th The control is better south of Cape Horn where pressure is too low in trial, but the trough at 40°W is better handled in the trial.

Fig 20 - VT 29th The large errors in the trial are due to the incorrect deepening of the low east of the Antarctic Peninsula. There were no significant difference elsewhere.

Fig 21 - VT 30th The previous days errors are reversed. The control is much too deep east of the Antarctic Peninsula. However further north, the trial is in error in having the flow too cyclonic

Fig 22 - VT 31st Again the control is much too deep east of the Antarctic Peninsula.

4.6 Impact on wave model

The ocean wave model at the UK Met Office is driven by surface winds from the atmospheric model. Because equilibrium wave height is proportional to wind-speed squared, and because wave models retain a memory of the past wind field through the presence of 'swell' energy, the wave model is a sensitive indicator to changes in the surface wind field of the atmospheric model.

A small signal was detected in the wave model analyses. Figure 23 shows the instantaneous wave height differences (trial - control) at 18UTC on 25th March. The contour interval is 0.2 m for wave height with shading of the .2-.6, .6-1.2 and >1.2 metre bands. We see small differences in the tropics associated with swell. Four areas in the latitude band 0-30°S have trial wave heights up to 0.5 metre higher as a result of the differing evolution of systems in the southern hemisphere storm belt at an earlier stage in the experiment.. The major impact in wave height is co-located with the differences in wind-speed (not shown) and is in regions where wind-speed and wave-height are highest, namely in the southern hemisphere storm belt south of 45°S. Some of the differences in the storm belt are clearly associated with a displacement of the synoptic features. There is no means of verifying the differences.

Trial mean wave heights were only 2 cm different (lower) from control . However point-wise differences were as much as 2 m. The full details are given in Table 5.

	Scatterometer wind trial	Control	Difference	
Wave height				
max	11.34	11.47	2.0	-1.9
mean	1.75	1.77	-0.014	
Wind-speed				
max	27.5	28.9	10.1	-8.5
mean	6.68	6.74	-0.063	

Table 5 : Mean and extreme differences between trial and control wave height fields and the associated wind speed field at 18UTC 25th March - units metres for wave height and m/s for wind speed

5. Performance of Scatterometer winds in a Regional Model Context

A northern hemisphere impact might be more likely within the higher resolution regional model where advantage could be taken of the small scale information that is seen in the scatterometer wind fields. Such a trial required the recoding of the derived increment calculation, discussed in section 3.2, so that it is applicable to a limited area domain. This has recently become available with build 3.3 of the unified model. A larger impact might also be found in the autumn, when the sea area and hence scatterometer wind coverage in the northern hemisphere is a maximum.

The limited area model was not part of the parallel trial. A few reruns of cases where scatterometer winds might have been beneficial have yet to yield a significant impact. However, none of these cases could be run with the benefit of derived pressure increments. Further trials of scatterometer winds in the LAM will be the subjective of future work.

Hammon and Wilson (1993) have suggested that many of the LAM rainfall evolution errors can be traced back to analysis deficiencies. Terry Davies (personal communication) has noted that both jet level errors and surface or low level errors are contributory to model evolution errors. He has studied one case from a data time of 12UTC 21st July 1993 where the low level advection was much too strong and resulted in a major timing error in the passage of a frontal system across the UK. If only scatterometer winds had been available!

At DNMI, Breitwik el al (1993) have found a rather small average, but occasionally significant, positive impact in the Norwegian LAM. The Norwegian area of interest is rather further north in general, and the analysis for their domain does suffer as much from the North Atlantic data drop-out (see Figure 2).

6. Performance of Scatterometer winds for tropical systems

Another area where the scatterometer occasionally provides information not previously obtainable, is in defining tropical systems. The global model has not got the resolution to define these adequately but does represent them as weaker features on a larger scale than in reality. Despite this, extremely useful forecasts of cyclone movement can be obtained. Conventional data sources are often lacking in the vicinity of tropical systems and we rely on manual intervention based on tropical storm strength and position messages. Alas during the trial, there was not a useful match between tropical systems and ERS-1 overpass.

One system, Tropical Cyclone Cecil was seen by ERS-1 during its growth phase in September 1993. Figure 24 compares the surface wind fields around tropical storm Cecil as depicted by the scatterometer wind observations (a) and the model background interpolated to observation points (b). We see that the observation suggest that the model background has located the centre rather too far to the north-west and is significantly too weak on the northern and eastern flank. A few obviously incorrect aliases have been chosen near the centre of the system. The observations also show an apparent convergence line to the rear of the system, which one might also suspect to be the result of a de-aliasing problem. However, Quilfen et. al. (1994) have noted this on several other systems and believe it to be a real feature created by non-linear interactions between the symmetric vortex and

environmental conditions. The same authors also note that the scatterometer observations never go beyond 25 m/s even though estimated winds have been as high as 70 m/s. The problem is suspected to be partly due to inadequacies in the retrieval model and partly resolution. In a global assimilation context this deficiency is probably of no consequence.

Figure 25 shows the model analysed surface wind field at 00UTC 24th Sept 1993 with scatterometer winds included (a) and a comparison background field (b) together with the difference (c). There were no other observations in the vicinity of the system so the difference can confidently be attributed to the scatterometer data. The analysis has the system further south and has stronger winds on the northern flank as observed. The impact was not retained beyond the first day of the forecast in this instance.

Hall et. al. (1993) reviewed the operational practices for use of 'bogus' data in the context of tropical cyclones in the UK global model. They noted that the usual practices are either to insert bogus winds at several levels up to 500 hPa with tangential directions except at 850 hPa where a 20° backing is allowed to induce convergence or alternatively for cases of mis-positioning to take both temperature and wind information from the model's incorrectly forecast system and adjust the position according to satellite image based advisories. It is not surprising therefore, that only modest success is obtained from simply using surface data, given that the vertical spreading functions and mass/wind couplings in the assimilation algorithms are not specifically tuned for tropical systems.

7. Conclusions

The southern hemisphere results discussed in section 3 are very impressive, with substantial reductions in rms errors (by as much as 10%) for the surface and low level height at all forecast ranges and modest reductions in temperature and wind rms errors. The subjective assessment discussed in section 4 provides further evidence for the usefulness of the scatterometer winds. The results clearly show that the data would make a valuable contribution to the operational forecast system. Since ERS-1 scatterometer winds started contributing to the operational observing system, the forecasters in the Central Forecast Office have noted a considerable improvement in southern hemisphere analyses, to the extent that they no Ionger think it necessary to intervene with bogus data. This improvement in part must stem from the use of scatterometer wind data. It is interesting to note that the ECMWF experience has not been so encouraging. Hoffman (1993) showed very little impact in a global study using the ECMWF system and more recently Stoffelen et. al. (1994) have performed further experiments using better wind retrieval, quality control and ambiguity removal with a similar disappointing result. This demonstrates that the assimilation technique is perhaps just as important as the observations being assimilated.

It might be argued that a null result outside the southern hemisphere implies that there is no call for scatterometer wind data north of 30°S. Clearly, the model background is better in the northern hemisphere so on average observations are less valuable, other data sources (eg ships) are more likely to make scatterometer wind observations redundant and as pointed out in section 2.2 at best the impact would be only a quarter of that found in the southern hemisphere based on data volume considerations. However even if it is difficult to see an impact in the northern hemisphere statistics, we should still expect improvements in

occasional cases, where the scatterometer winds (which are clearly of good quality) identify and correct significant errors in the model background in areas devoid of conventional data sources. The trial was of insufficient length to identify such a case, but there is some expectation that a more significant impact will be felt in the higher resolution regional model where advantage could be taken of the small scale information that is seen in the scatterometer wind fields.

The performance with regard to tropical systems has not been fully evaluated. Coincidence of the observations with cyclone positions is rarely achieved and when the systems are observed by the ERS-1 satellite we still have considerable problems assimilating the data without supporting upper air information being provided by our forecasters. Nevertheless, the winds are clearly providing a valuable input into the subjective forecasts of tropical systems.

Acknowledgements

The following contributed to this work. David Offiler (scatterometer algorithm development), Geoff Smith (validation), Andrew Lorenc (project leader) and Philip Andrews (development of balanced increment code)

Figures

Fig. 1 Typical daily coverage- the ERS-1 swath where data was available during 21 March 1993

Fig. 2 Scatterometer wind distribution; cumulative data density during period 19-28 March as a % of maximum

Fig. 3 Typical analysis difference; (trial-control); 10 m wind; VT 12UTC 28 March 1993

Fig. 4 Typical analysis difference; (trial-control); 850 hPa wind; VT 12UTC 28 March 1993

Fig. 5 Typical analysis difference; (trial-control); pmsl; VT 12UTC 28 March 1993

Fig. 6 Typical forecast difference; (trial-control); pmsl; T+72; VT 12UTC 31 March 1993

Fig. 7 Zonal mean latitude-height plot of RMS analysis temperature difference;sea points only; (trial-control); 10 analyses; 19-28 March 1993

Fig. 8 Zonal mean latitude-height plot of RMS analysis vector wind difference; sea points only; (trial-control); 10 analyses; 19-28 March 1993

Fig. 9 RMS analysis difference; (trial-control); 10 m wind; 10 analyses; 19-28 March 1993

Fig. 10 RMS analysis difference;(trial-control); 850 hPa wind; 10 analyses; 19-28 March 1993

Fig. 11 RMS analysis difference;(trial-control); pmsl; 10 analyses; 19-28 March 1993

Fig. 12 T+72 forecast surface pressure verification comparison (trial v control) for South Atlantic sector

Figs. 13-22 Sequence of South Atlantic forecast comparison with verification for T+72 plus forecast differences from verification and each other.

Fig. 23 Instantaneous wave height differences (trial - control) at 18UTC on 25th March.

Fig. 24 Surface wind flow around tropical storm Cecil, 24th Sept 1993, a) scatterometer wind observations and b)model background interpolated to observation points.

Fig. 25 Model surface wind fields at 00UTC 24th Sept 1993, a) analysed with scatterometer winds, b) background T+6 and c) difference.

References

Andrews, P.L. and R.S. Bell, 1993, Balanced surface pressure and temperature increments derived from wind increments in the AC assimilation scheme, *Met.O.(FR) Tech. Rep. No. 52*

Breitwik, L-A., B. Haugse and M. Homleid, 1994, Results from assimilation of ERS-1 scatterometer wind information in an operational limited area weather forecast model, *Proc. 2nd ERS-1 Symposium Space at the Centre of our Environment, Hamburg - Oct. 1993, ESA SP 361, pp.201-206*

Bell, R.S., 1994, Operational use of ERS-1 products in the Meteorological Office, *Proc. 2nd ERS-1 Symposium Space at the Centre of our Environment, Hamburg - Oct. 1993, ESA SP 361, pp.195-200*

Bell, R.S. and M. Holt, 1993, Use of ERS-1 wind and wave products in operational meteorology, *Proc. 1st ERS-1 Symposium Space at the Centre of our Environment, Cannes - Nov. 1992, ESA SP 359 pp.705-709*

Hall, C.D., J.C.R. Hunt and A.M.Radford, 1993, Forecasting Tropical Cyclones and near surface wind conditions, *Proc. ICSU/WMO Internat. Symposium on Tropical Cyclone Disasters, Beijing - Oct 1992*

Hammon, O. and C.W.Wilson, 1993, Poor precipitation forecasts for the Limited Area Model, *Met.O.(FR) Tech. Rep. No. 74*

Hoffman, R.N., 1993, A preliminary study of the impact of the ERS 1 C band scatterometer wind data on the European Centre for Medium-Range Weather Forecasts global data assimilation system, *J. of Geophys. Res., **98**, No. C6, pp.10233-10244*

Lorenc, A.C., R.S. Bell and B. Macpherson, 1991, The Meteorological Office Analysis Correction data assimilation scheme, *Quart.J.Roy.Met.Soc., **117**, 59-89*

Offiler,D., 1990, Wind fields and Surface Fluxes, *NATO ASI Series C:Math Phys Sci **298**, pp.355-374*

Quilfen, Y., K.B. Katsaros, B. Chapron, and H. Zhao, 1994, Surface wind and precipitation patterns in tropical cyclones observed with the ERS-1 scatterometer and with the special sensor microwave imager, *Proc. 2nd ERS-1 Symposium Space at the Centre of our Environment, Hamburg - Oct. 1993, ESA SP 361, pp.1117-1122*

Smith,S.G., and S.R.Waters, 1992, Statistics of ERS-1 scatterometer winds for March 1992 including a comparison with ship observations, *Met.O.(CF) Monitoring Note No.8*

Stoffelen, A. and D.L.T. Anderson, 1993, ERS-1 scatterometer data characteristics and wind retrieval skill, *Proc 1st ERS-1 Symposium Space at the Centre of our Environment, Cannes - Nov. 1992, ESA SP 359 pp.41-47*

Stoffelen, A., C.Gaffard and D.Anderson, 1994, ERS-1 scatterometer data assimilation, *Proc. 2nd ERS-1 Symposium Space at the Centre of our Environment, Hamburg - Oct. 1993, ESA SP 361, pp.191-194*

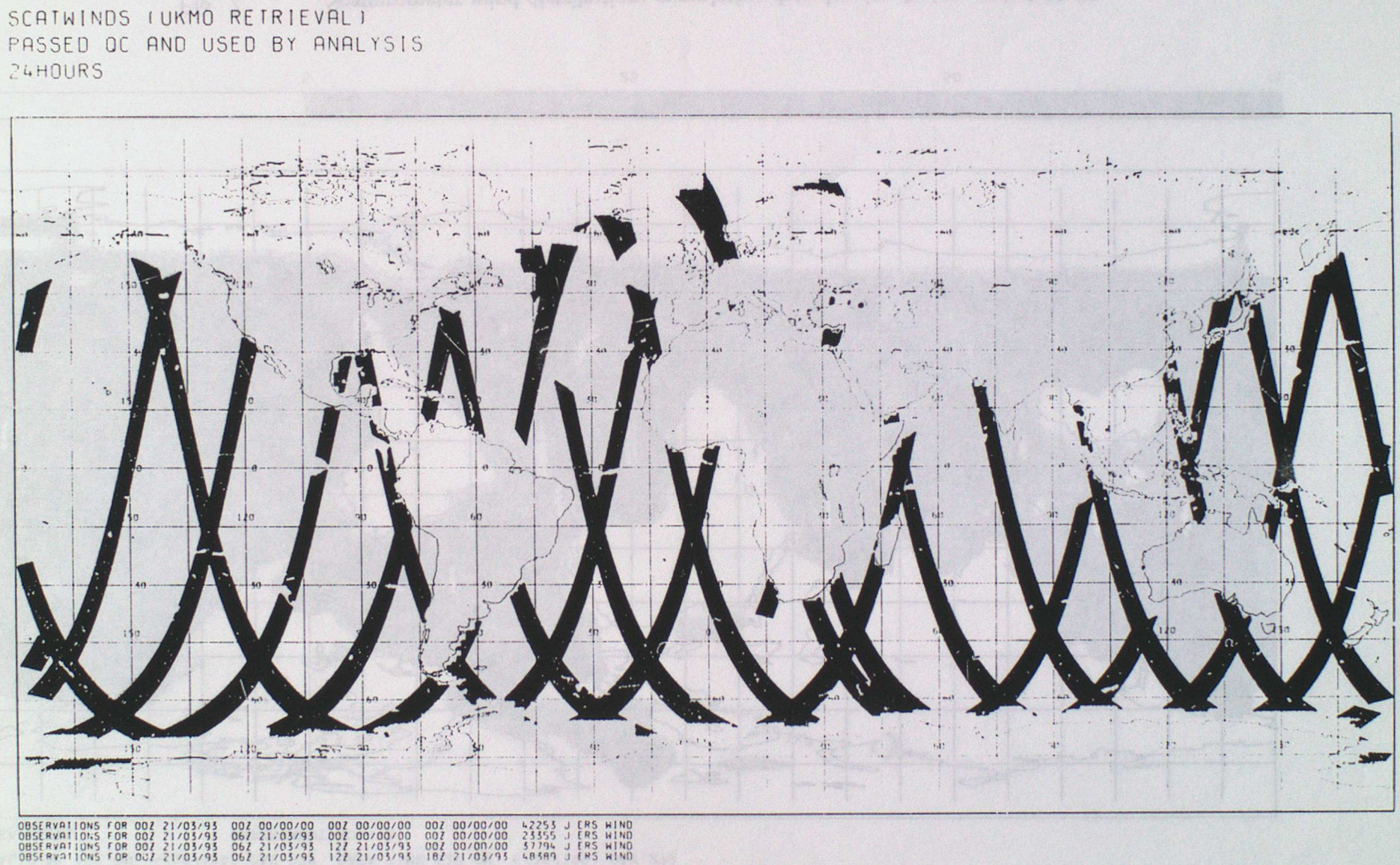

Fig. 1 Typical daily coverage- the ERS-1 swath where data was available during 21 March 1993

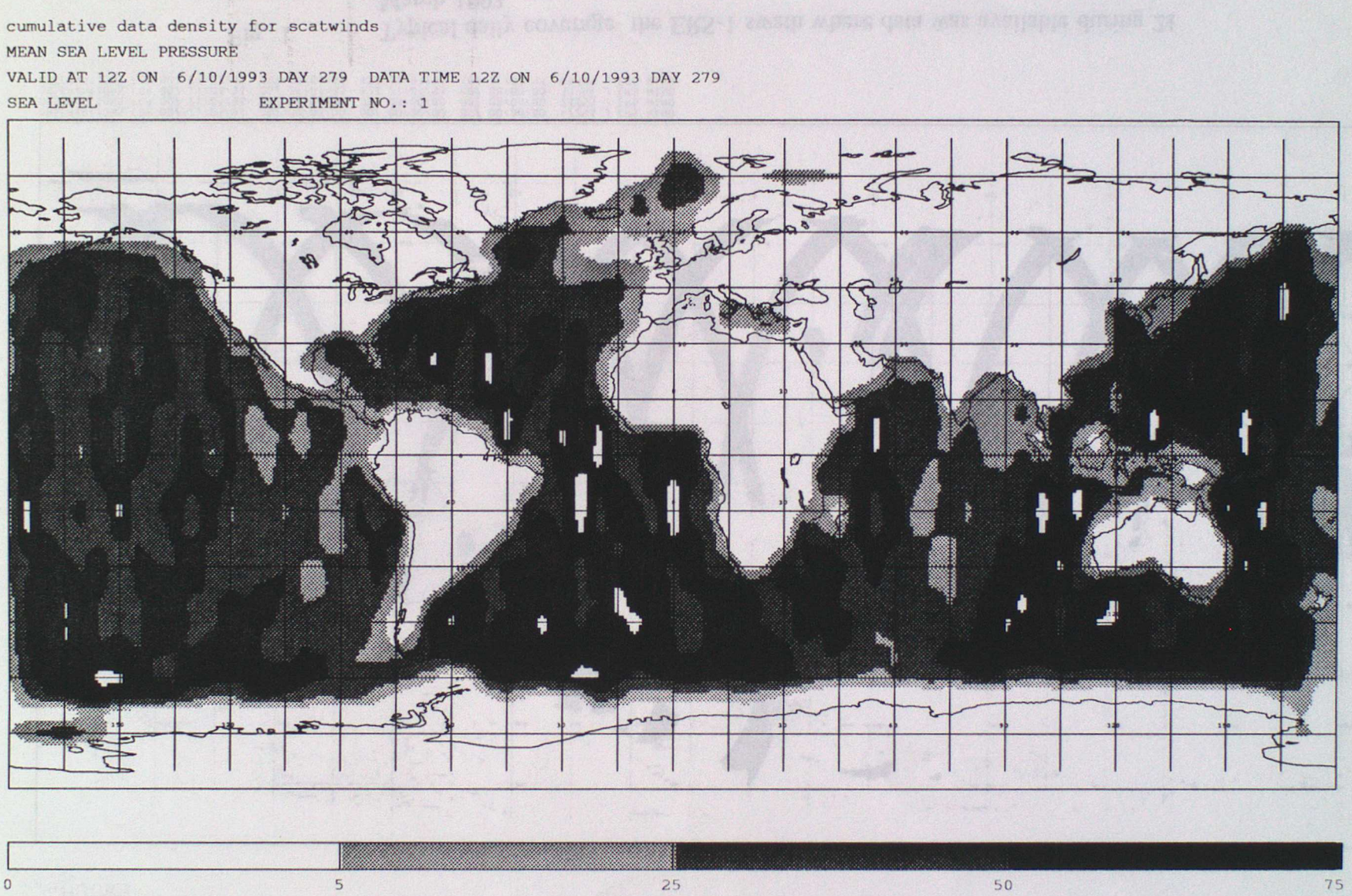

Fig. 2 Scatterometer wind distribution; cumulative data density during period 19-28 March as a % of maximum

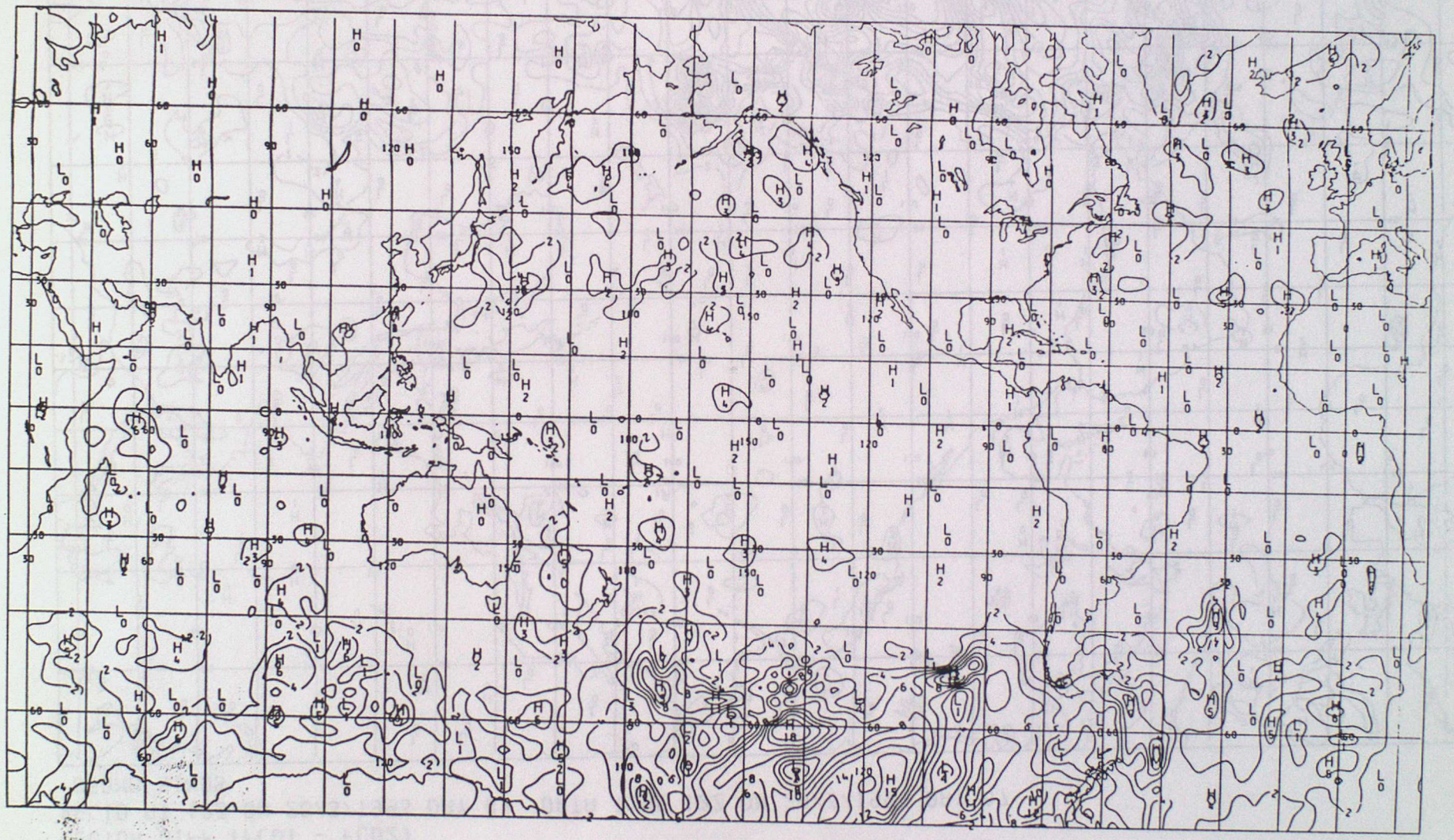

Fig. 3 Typical analysis difference; (trial-control); 10 m wind; VT 12UTC 28 March 1993

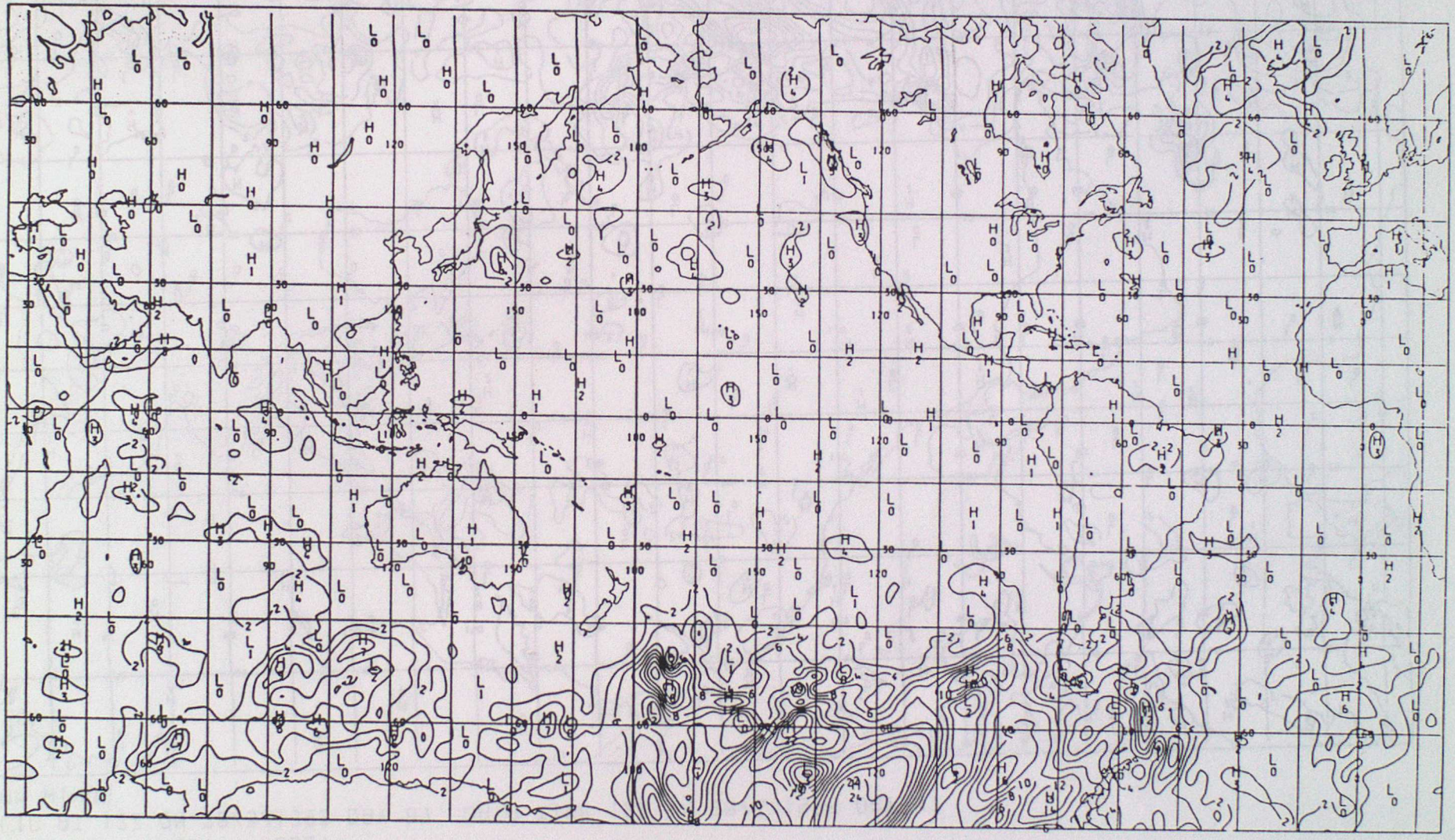

Fig. 4 Typical analysis difference; (trial-control); 850 hPa wind; VT 12UTC 28 March 1993

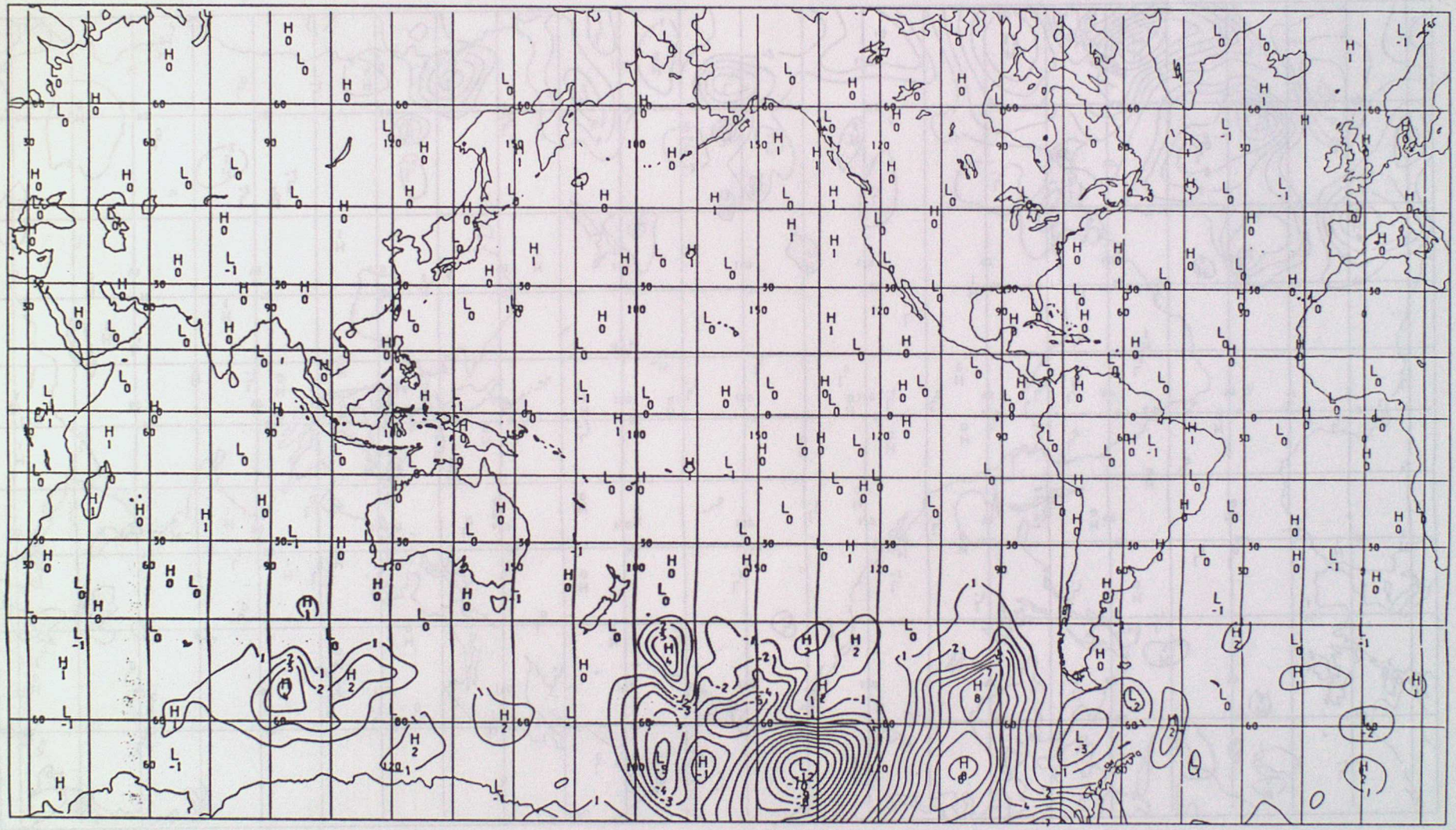

Fig. 5 Typical analysis difference; (trial-control); pmsl; VT 12UTC 28 March 1993

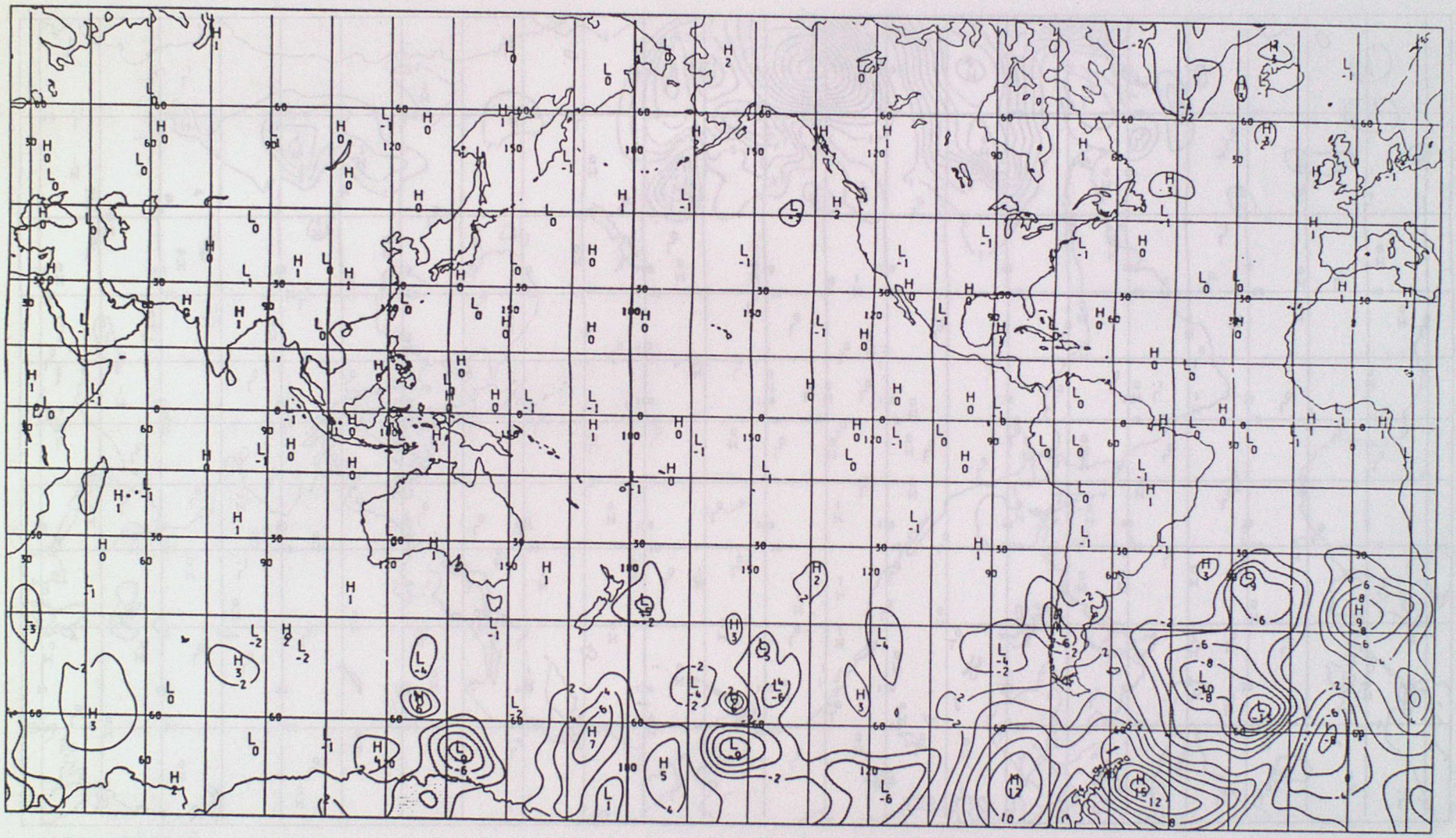

Fig. 6 Typical forecast difference; (trial-control); pmsl; T+72; VT 12UTC 31 March 1993

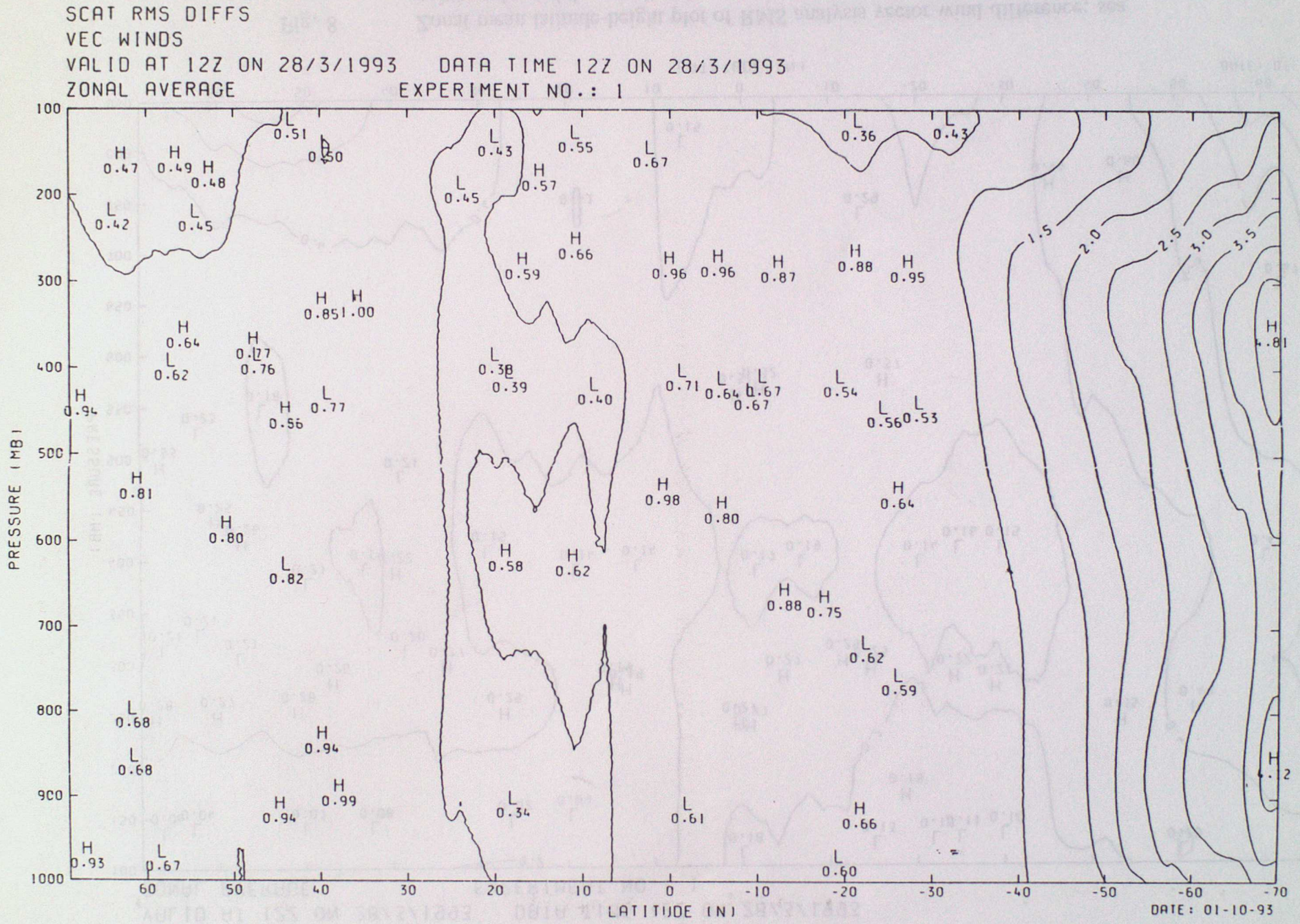

Fig. 7 Zonal mean latitude-height plot of RMS analysis temperature difference;sea points only; (trial-control); 10 analyses; 19-28 March 1993

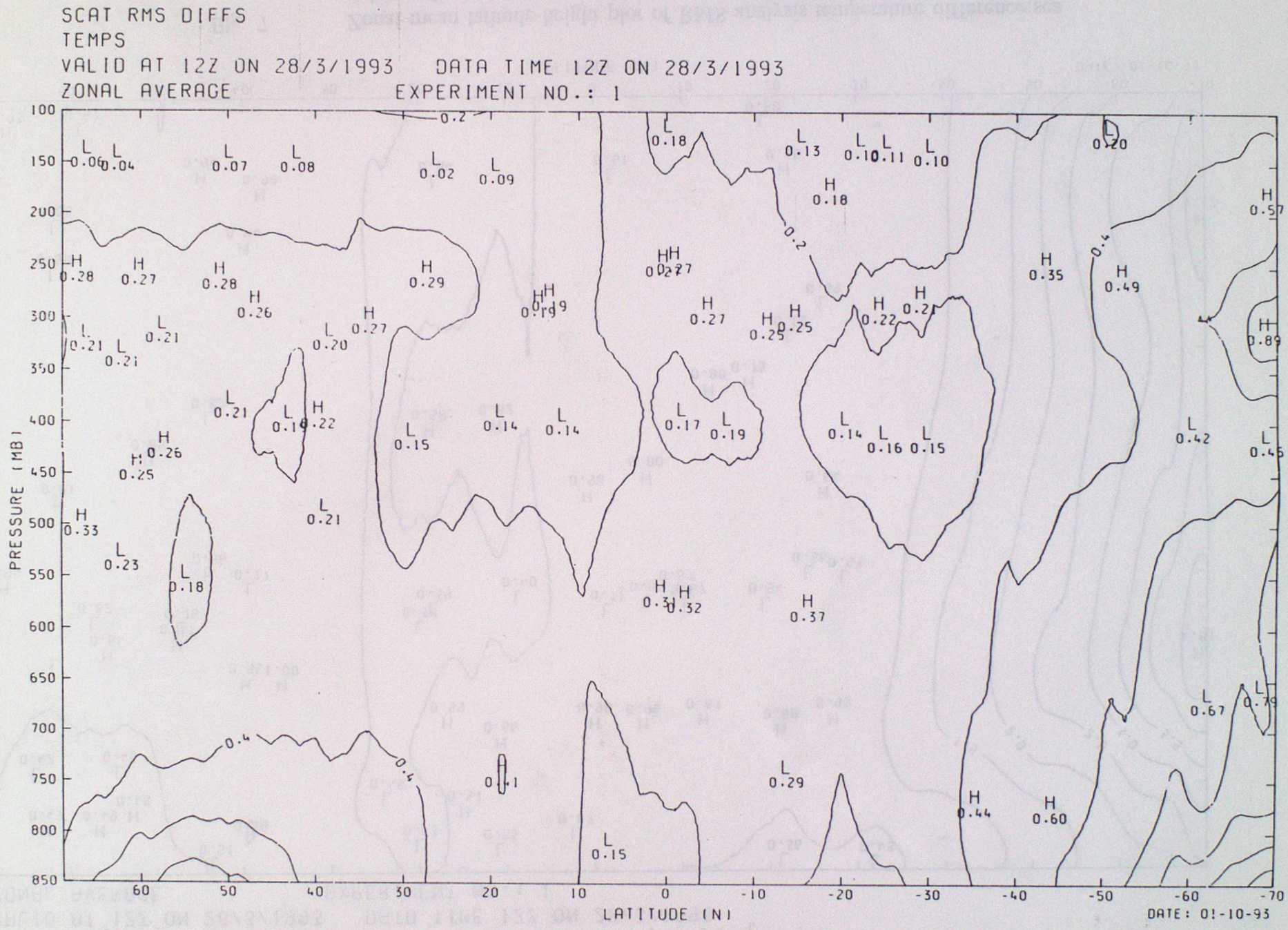

Fig. 8 Zonal mean latitude-height plot of RMS analysis vector wind difference; sea points only; (trial-control); 10 analyses; 19-28 March 1993

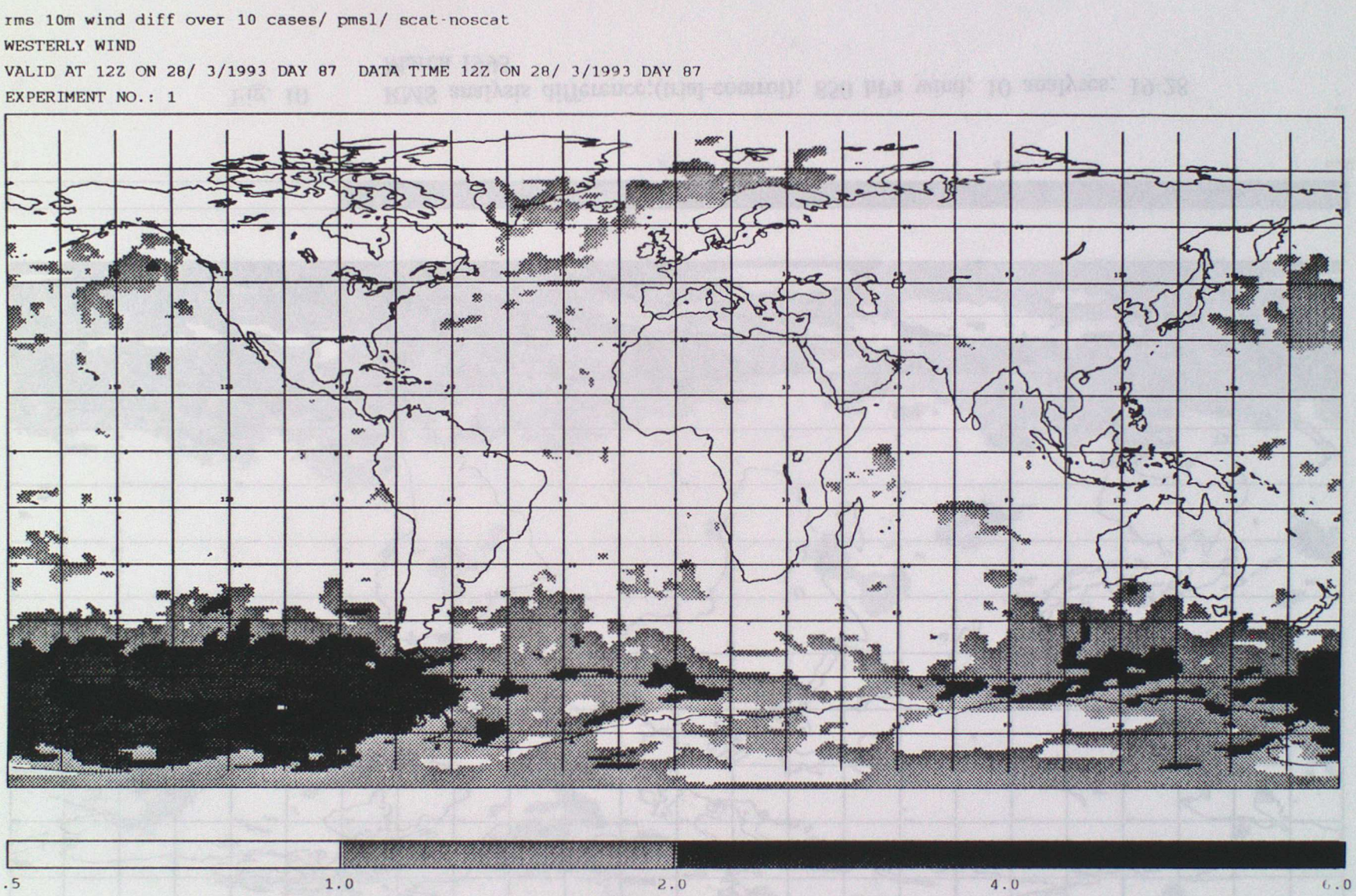

Fig. 9 RMS analysis difference; (trial-control); 10 m wind; 10 analyses; 19-28 March 1993

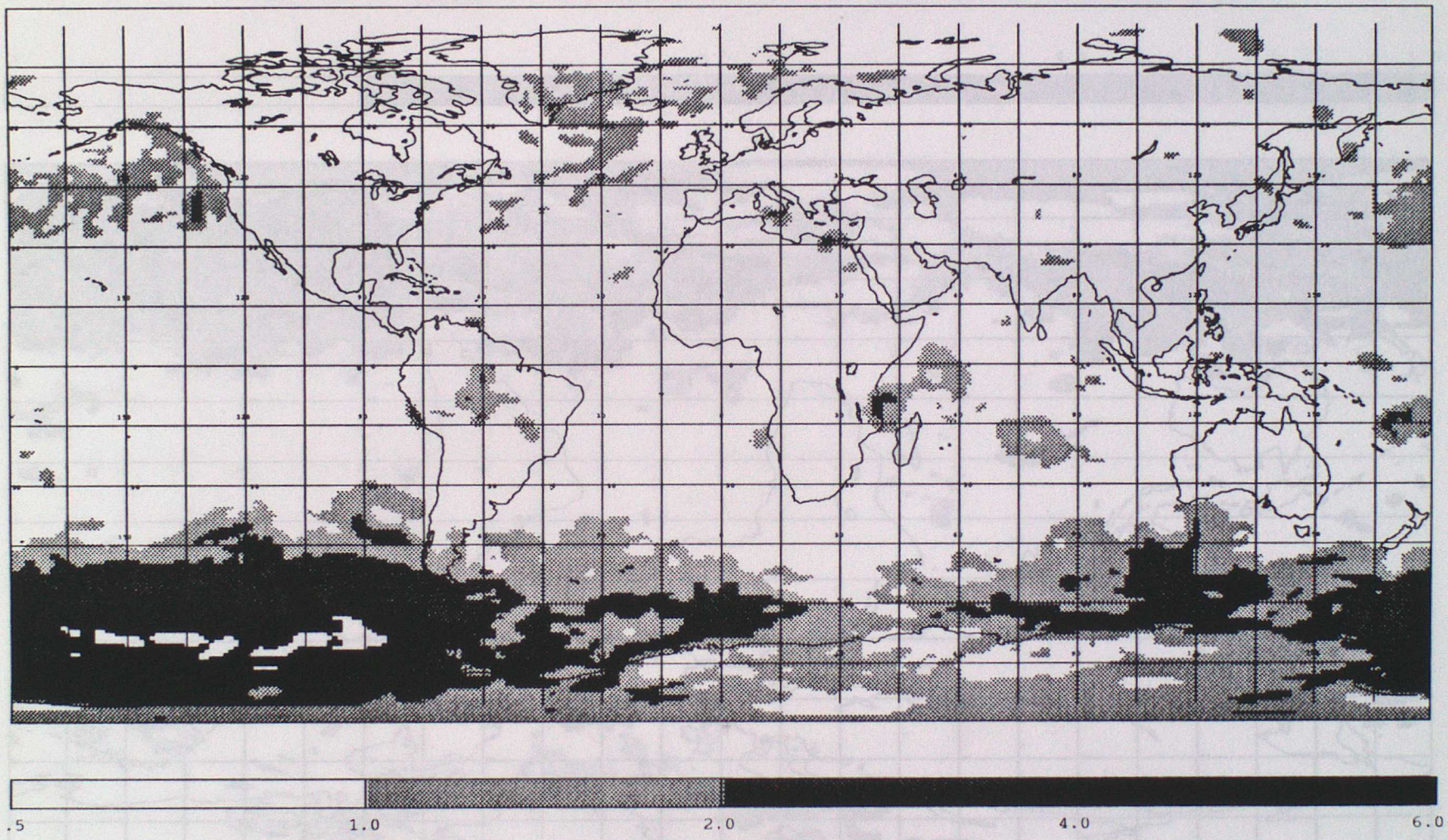

Fig. 10 RMS analysis difference;(trial-control); 850 hPa wind; 10 analyses; 19-28 March 1993

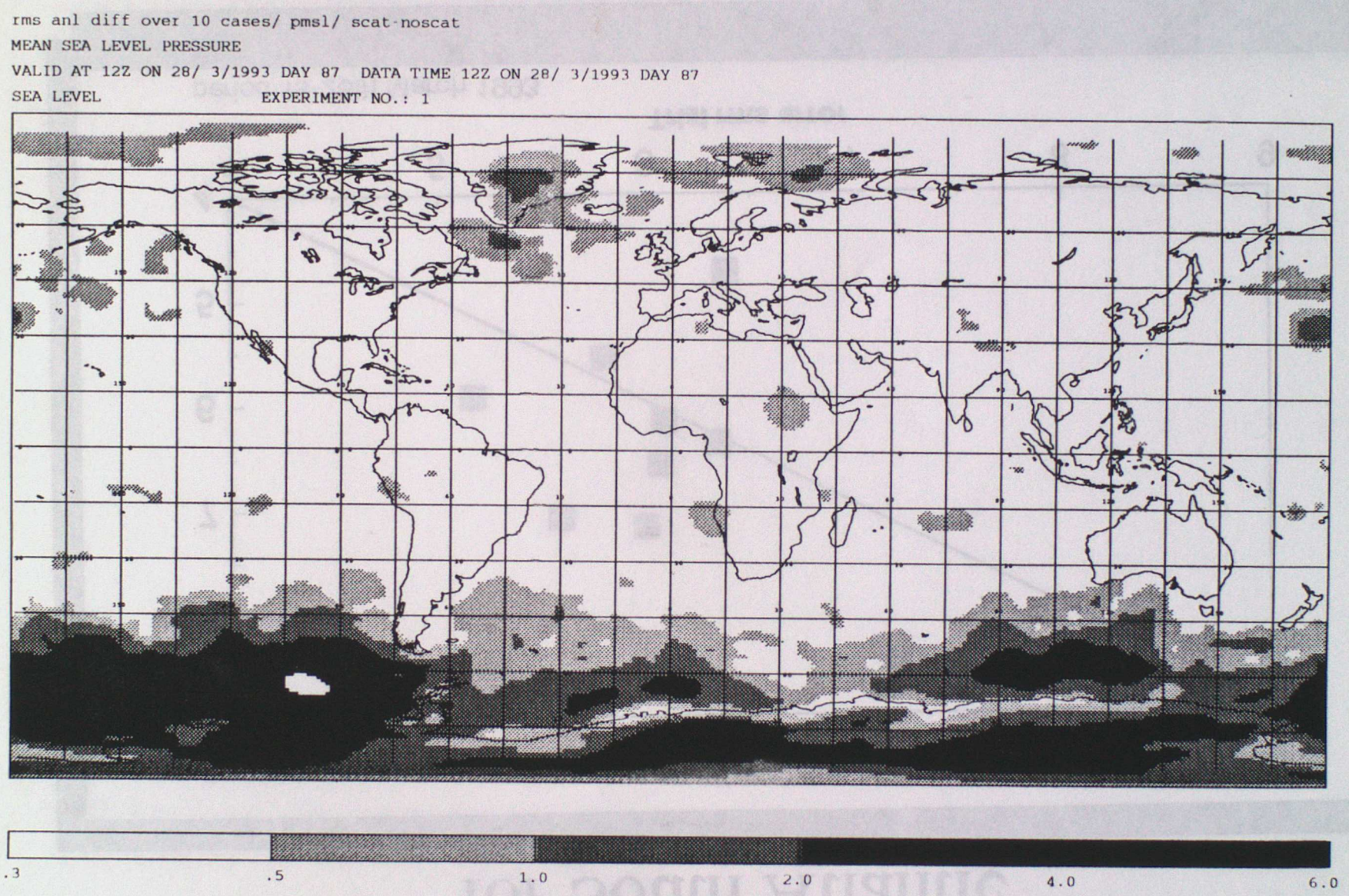

Fig. 11 RMS analysis difference;(trial-control); pmsl; 10 analyses; 19-28 March 1993

Comparison of 3 day surface pressure forecast verification for South Atlantic

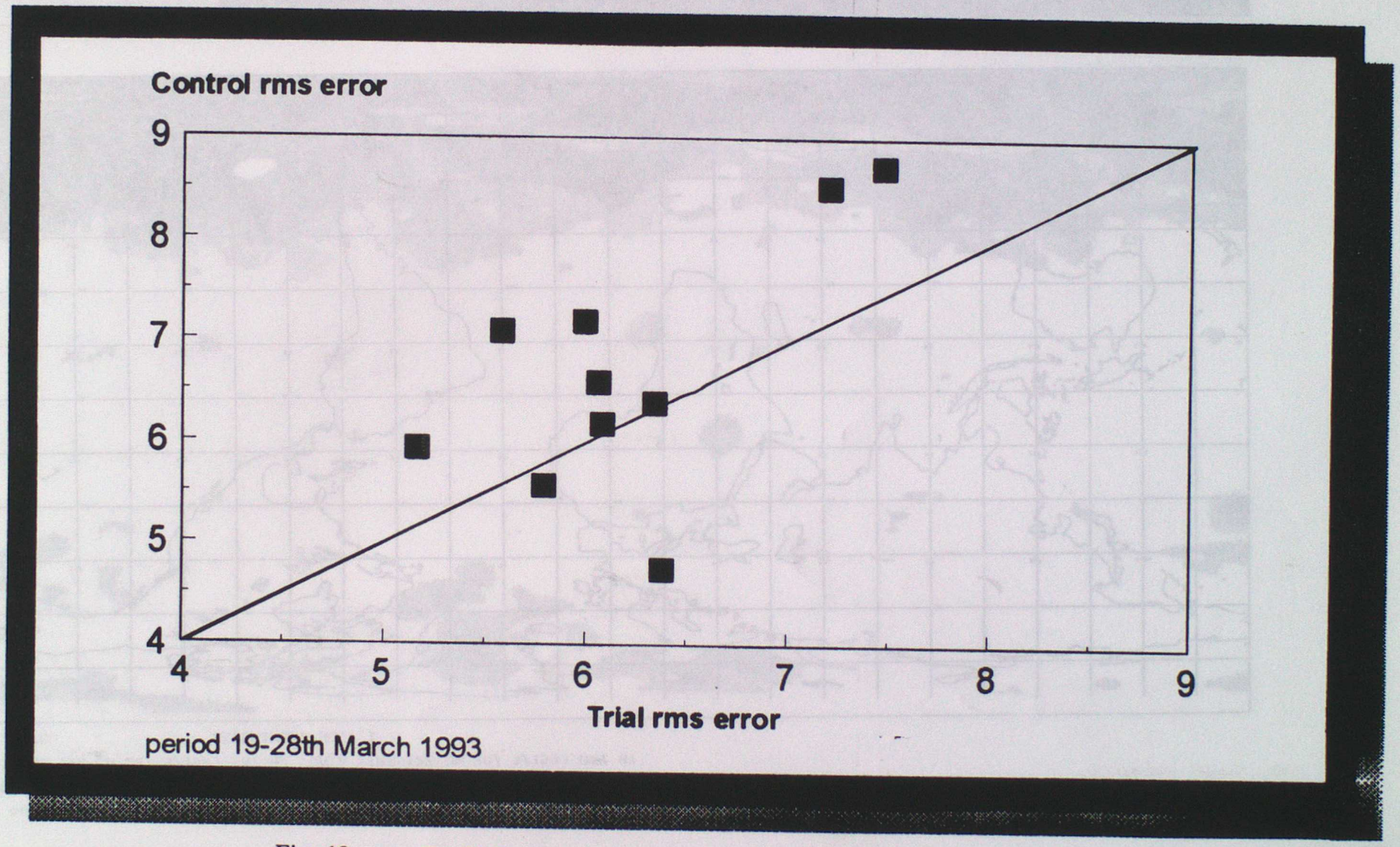

Fig. 12 T+72 forecast surface pressure verification comparison (trial v control) for South Atlantic sector

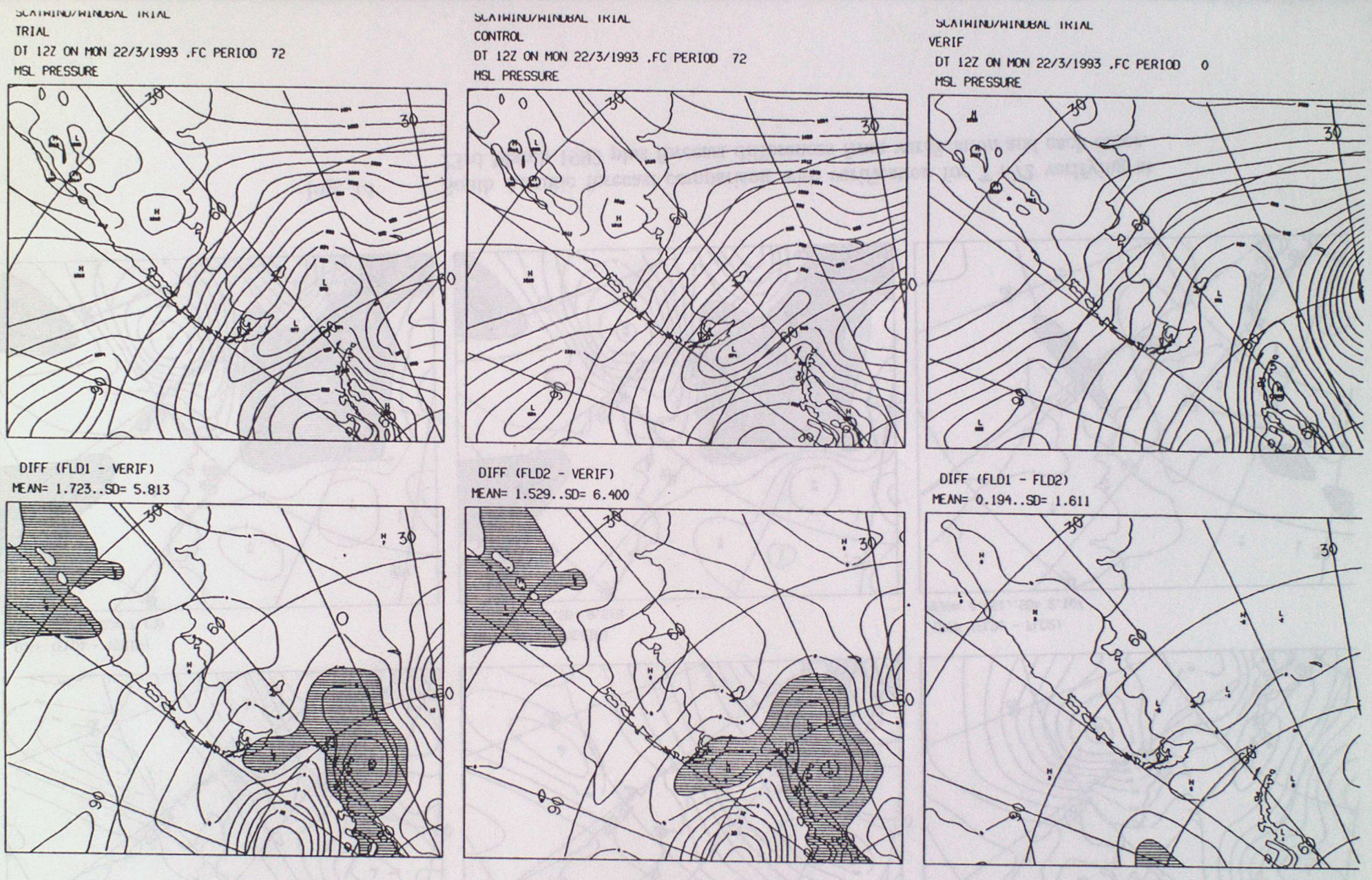

Fig. 13 South Atlantic forecast comparison with verification for T+72 verifying at 22nd March 1993 plus forecast differences from verification and each other.

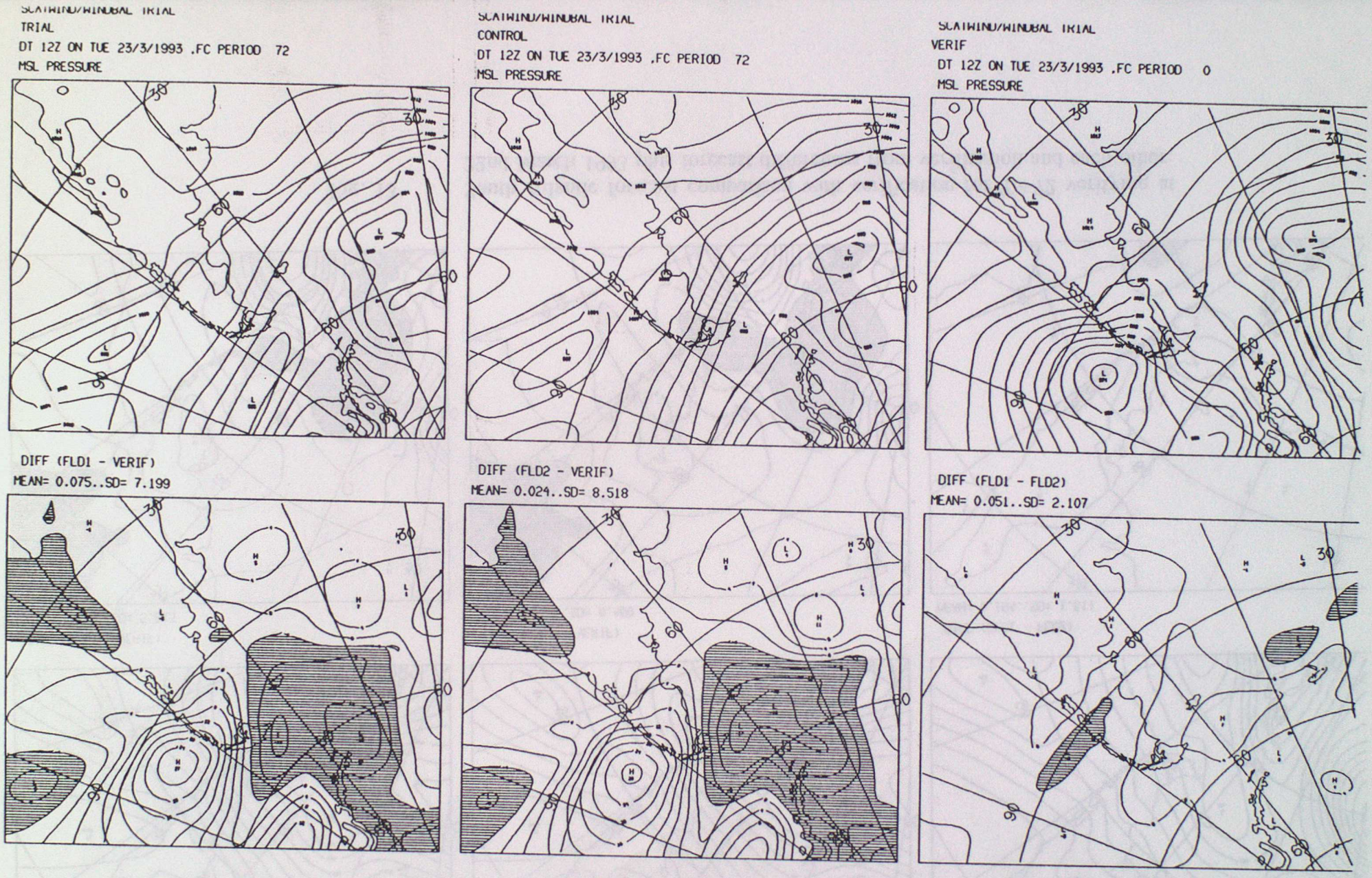

Fig. 14 South Atlantic forecast comparison with verification for T+72 verifying at 23rd March 1993 plus forecast differences from verification and each other.

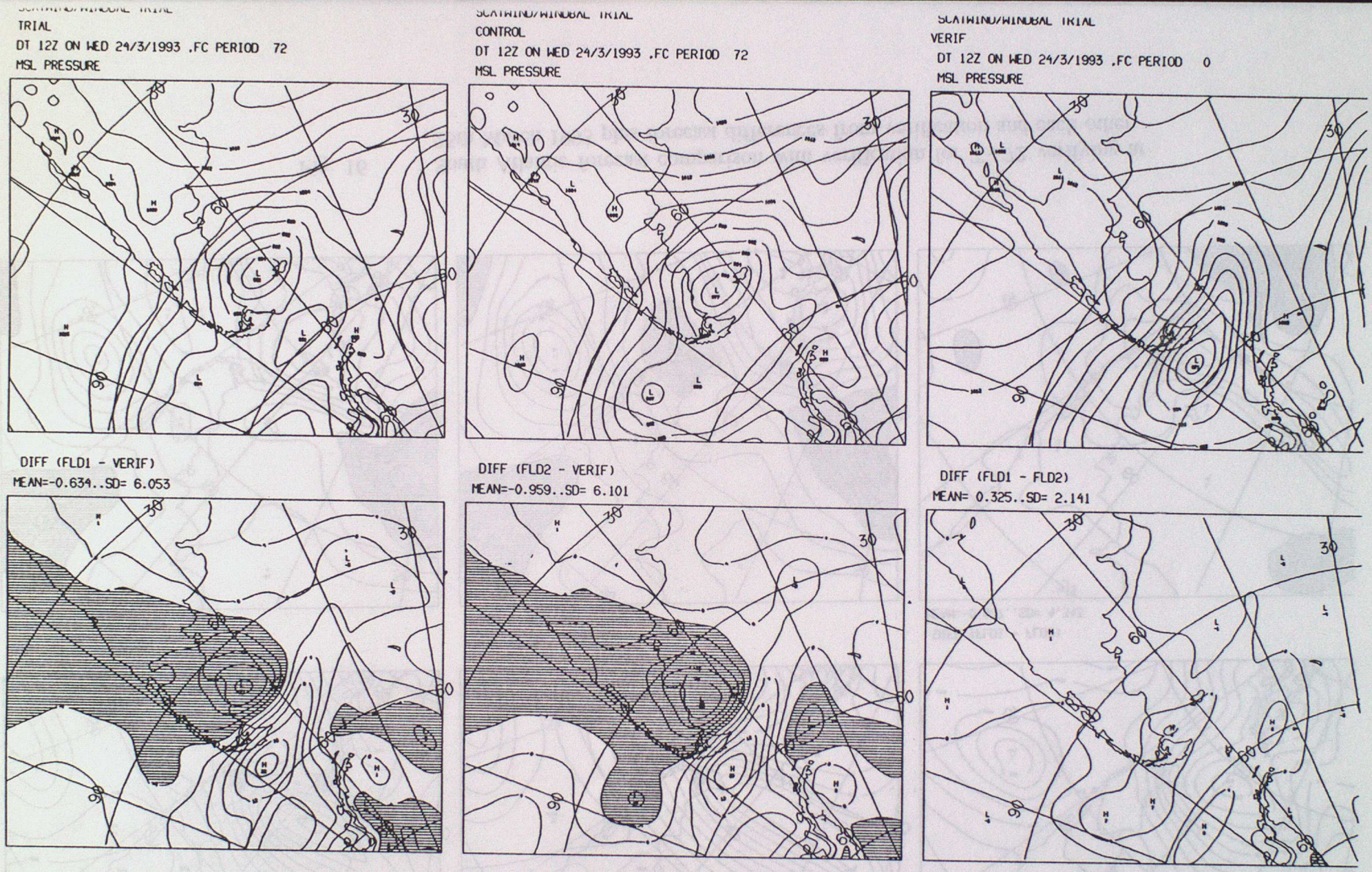

Fig. 15 South Atlantic forecast comparison with verification for T+72 verifying at 24th March 1993 plus forecast differences from verification and each other.

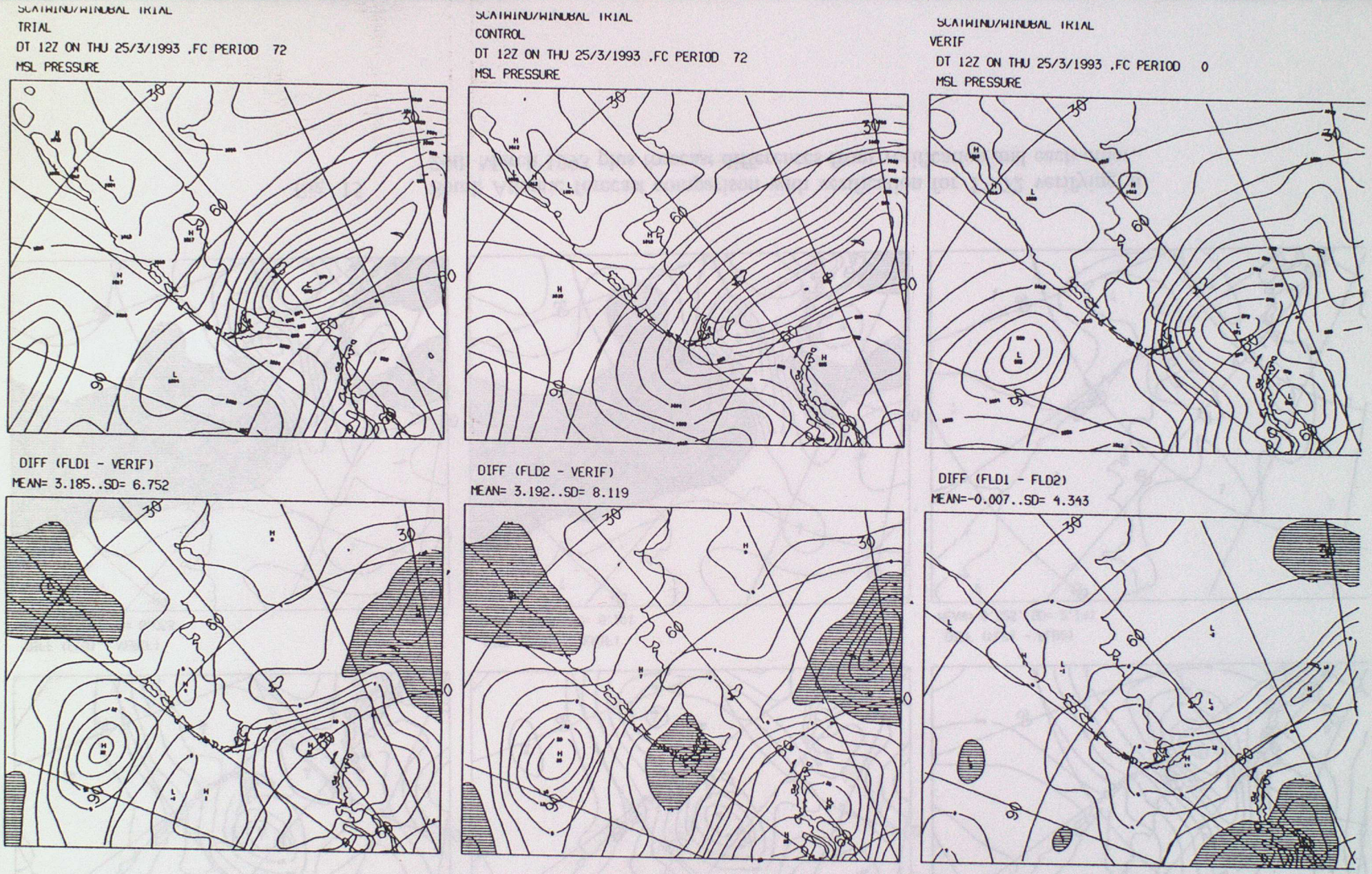

Fig. 16 South Atlantic forecast comparison with verification for T+72 verifying at 25th March 1993 plus forecast differences from verification and each other.

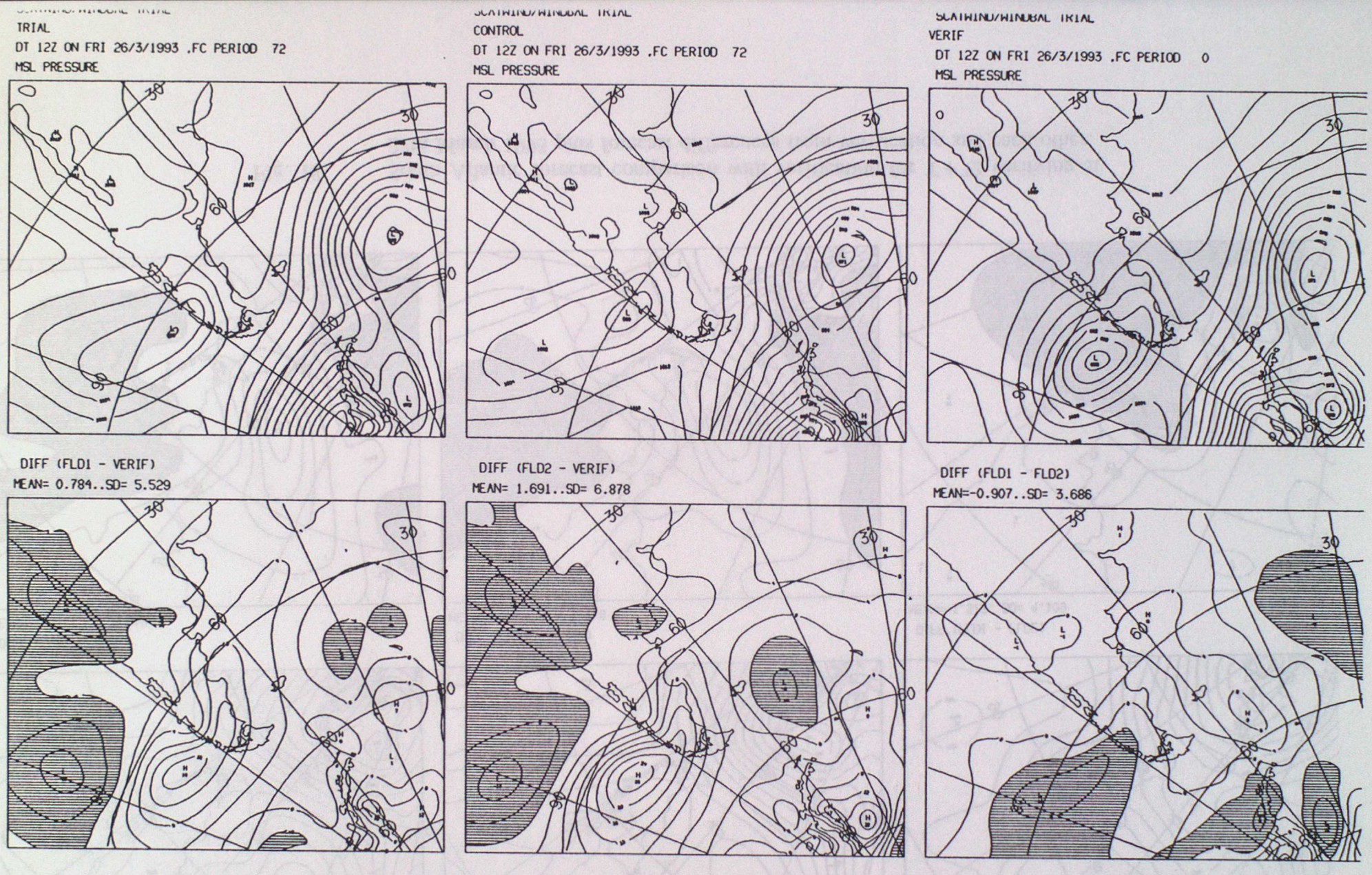

Fig. 17 South Atlantic forecast comparison with verification for T+72 verifying at 26th March 1993 plus forecast differences from verification and each other.

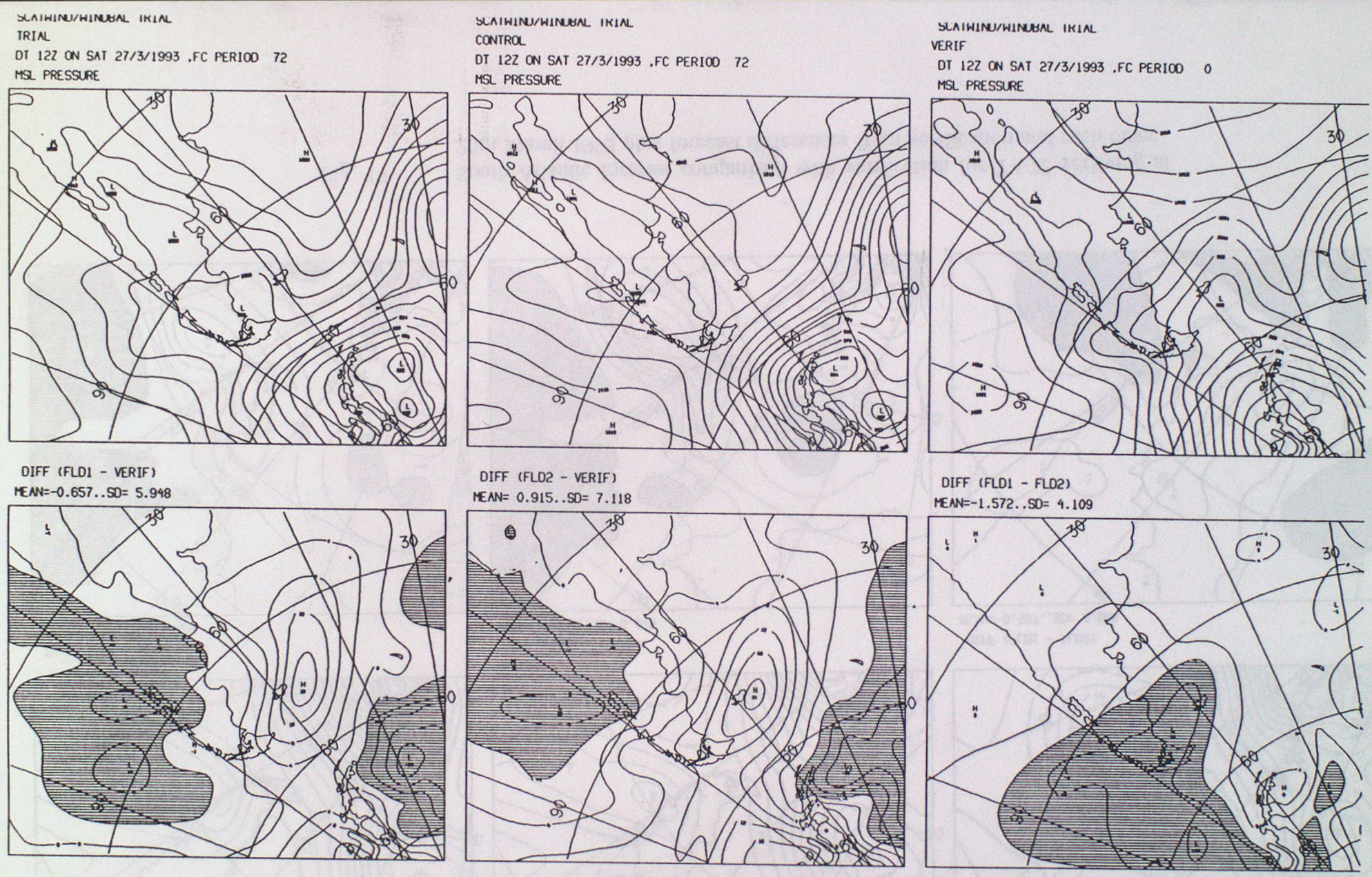

Fig. 18 South Atlantic forecast comparison with verification for T+72 verifying at 27th March 1993 plus forecast differences from verification and each other.

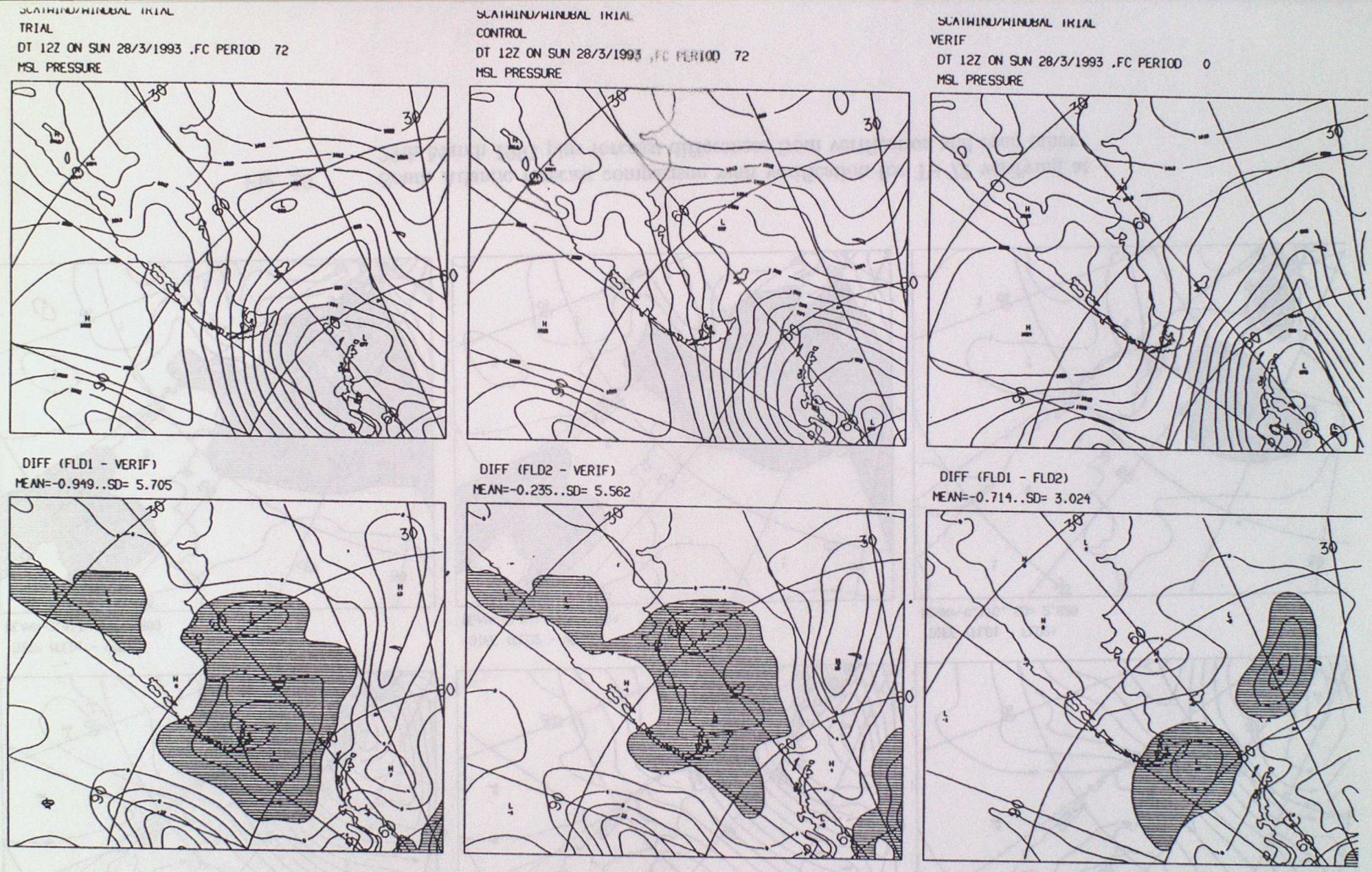

Fig. 19 South Atlantic forecast comparison with verification for T+72 verifying at 28th March 1993 plus forecast differences from verification and each other.

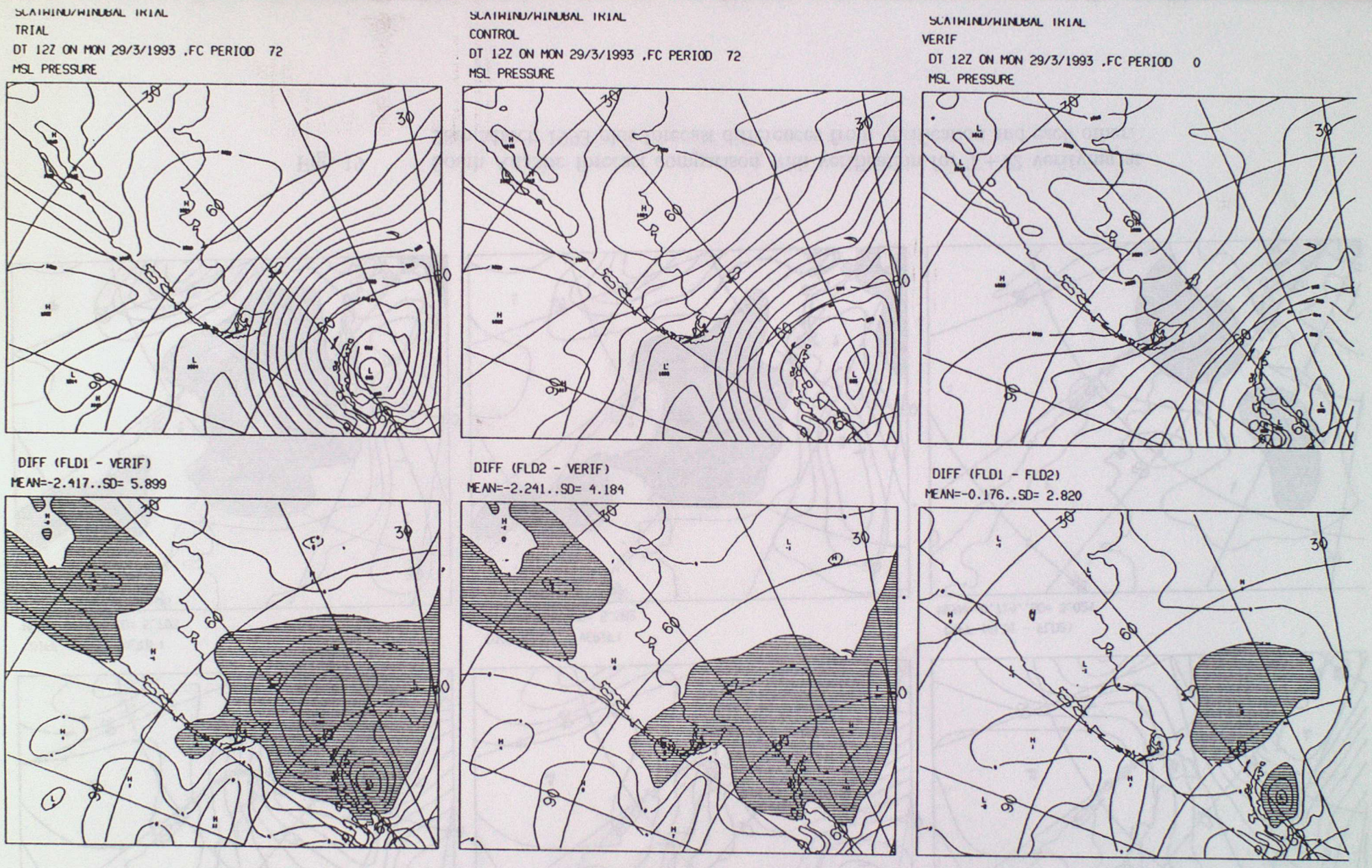

Fig. 20 South Atlantic forecast comparison with verification for T+72 verifying at 29th March 1993 plus forecast differences from verification and each other.

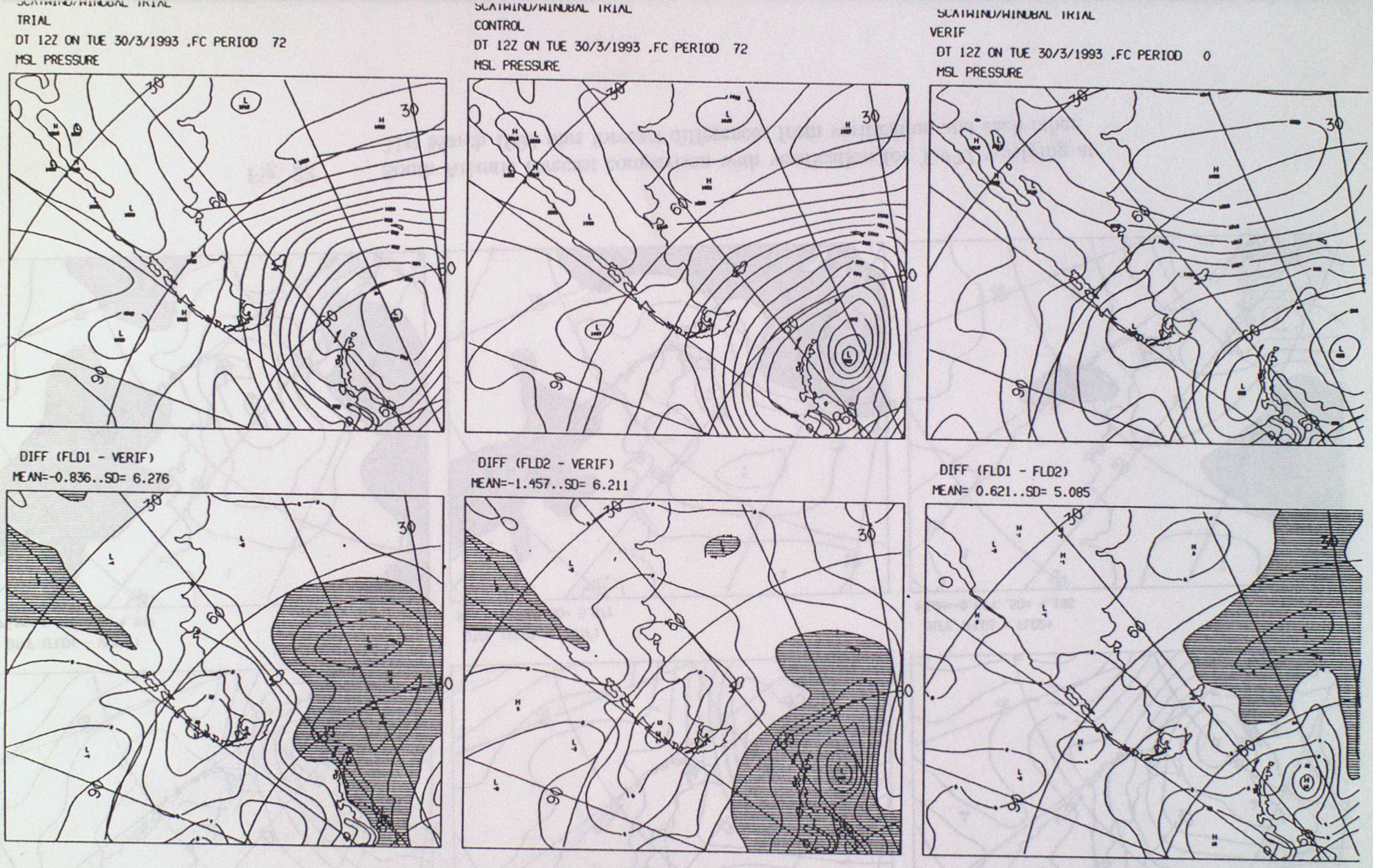

Fig. 21 South Atlantic forecast comparison with verification for T+72 verifying at 30th March 1993 plus forecast differences from verification and each other.

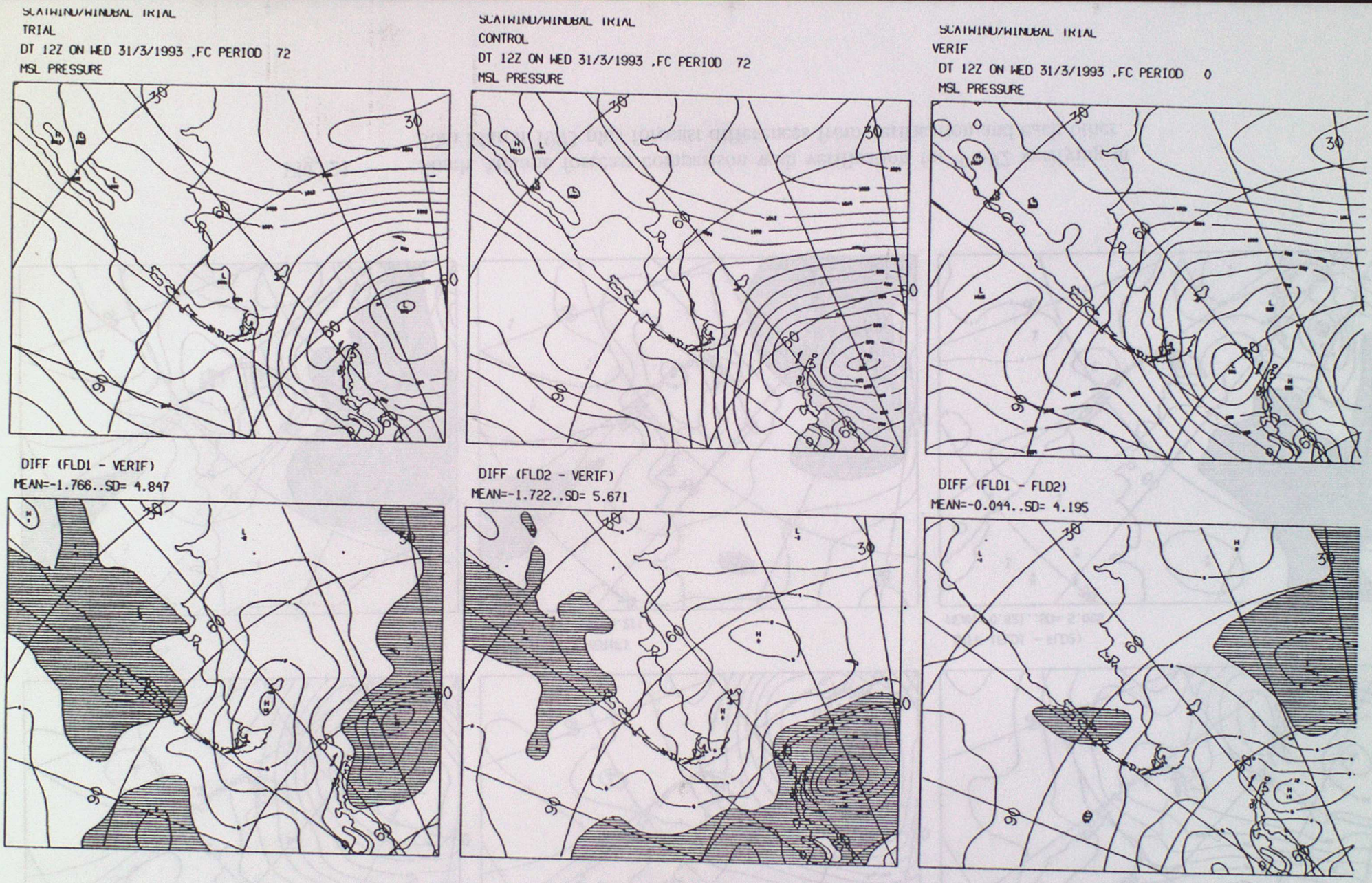

Fig. 22 South Atlantic forecast comparison with verification for T+72 verifying at 31st March 1993 plus forecast differences from verification and each other.

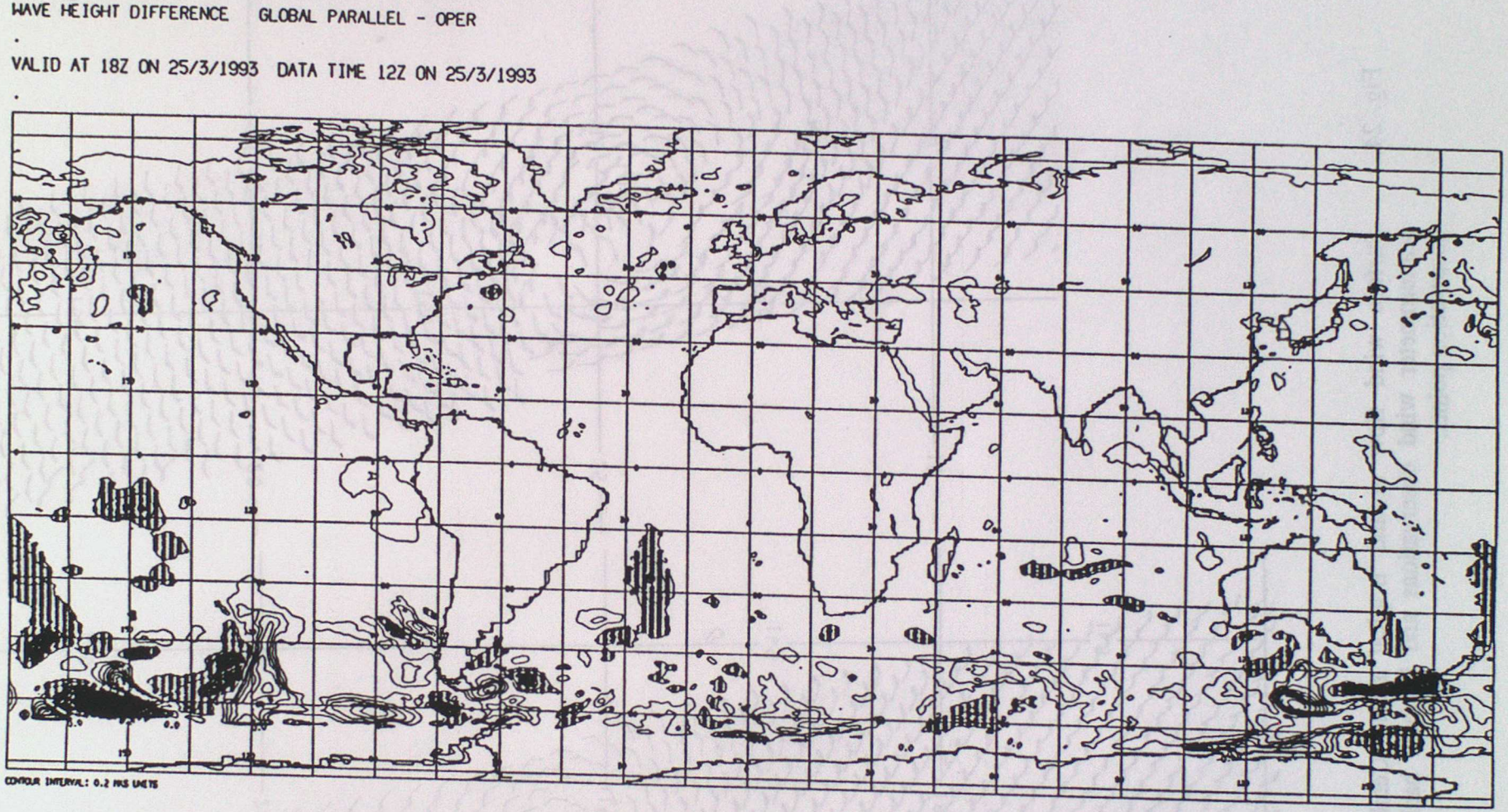

Fig. 23 Instantaneous wave height differences (trial - control) at 18UTC on 25th March.

Fig. 24 Surface wind flow around tropical storm Cecil, 24th Sept 1993, a) scatterometer wind observations and b)model background interpolated to observation points.

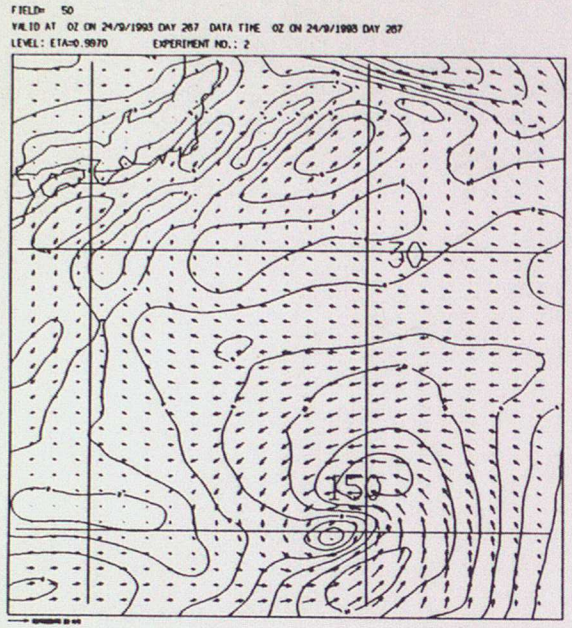

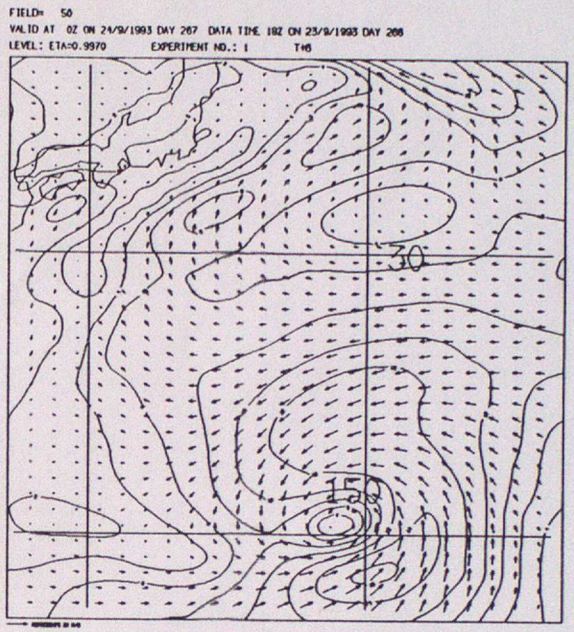

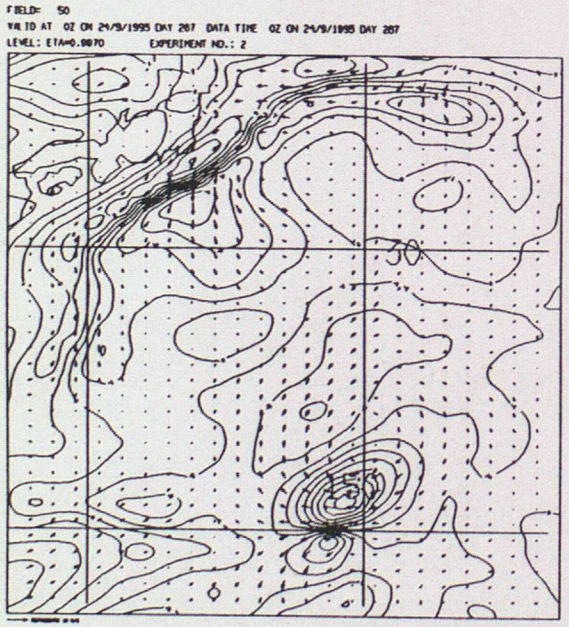

Fig. 25 Model surface wind fields at 00UTC 24th Sept 1993, a) analysed with scatterometer winds, b) background T+6 and c) difference.